Peer review history for:

Boadu A, Karpoormath R, Nlooto N. Pharmaco-phytochemistry of esters isolated from leaf extracts of *Spondias mombin* as potential antiviral agent. S Afr J Sci. 2024;120(7/8), Art. #14913. https://doi.org/10.17159/sajs.2024/14913

HOW TO CITE:
Pharmaco-phytochemistry of esters isolated from leaf extracts of *Spondias mombin* as potential antiviral agent [peer review history]. S Afr J Sci. 2024;120(7/8), Art. #14913.
https://doi.org/10.17159/sajs.2024/14913/peerreview

Reviewer I: Round 1
Date completed: 02 March 2024
Recommendation: Accept / **Revisions required** / Resubmit for review / Decline
Conflicts of interest: None

Does the manuscript fall within the scope of SAJS?
Yes/No
Is the manuscript written in a style suitable for a non-specialist and is it of wider interest than to specialists alone?
Yes/No
Does the manuscript contain sufficient novel and significant information to justify publication?
Yes/No
Do the Title and Abstract clearly and accurately reflect the content of the manuscript?
Yes/**No**
Is the research problem significant and concisely stated?
Yes/**No**
Are the methods described comprehensively?
Yes/No
Is the statistical treatment appropriate?
Yes/No/Not applicable/Not qualified to judge
Are the interpretations and conclusions justified by the research results?
Yes/Partly/No
Please rate the manuscript on overall contribution to the field
Excellent/**Good**/Average/Below average/Poor
Please rate the manuscript on language, grammar and tone
Excellent/Good/Average/Below average/Poor
Is the manuscript succinct and free of repetition and redundancies?
Yes/No
Are the results and discussion confined to relevance to the objective(s)?
Yes/No
The number of tables in the manuscript is
Too few/**Adequate**/Too many/Not applicable
The number of figures in the manuscript is
Too few/**Adequate**/Too many/Not applicable
Is the supplementary material relevant and separated appropriately from the main document?
Yes/No/Not applicable
Please rate the manuscript on overall quality

Excellent/Good/**Average**/Below average/Poor

Is appropriate and adequate reference made to other work in the field?

Yes/No

Is it stated that ethical approval was granted by an institutional ethics committee for studies involving human subjects and non-human vertebrates?

Yes/No/**Not applicable**

If accepted, would you recommend that the article receives priority publication?

Yes/No

Are you willing to review a revision of this manuscript?

Yes/**No**

Select a recommendation:

Accept / **Revisions required** / Resubmit for review / Decline

With regard to our policy on 'Publishing peer review reports', do you give us permission to publish your anonymised peer review report alongside the authors' response, as a supplementary file to the published article? Publication is voluntary and only with permission from both yourself and the author.

Yes/No

Comments to the Author:

The draft: Structures and anti-Rhino virus properties of 6-methylheptyl pentadecanoate and 6-1 methylheptyl 15-(1,2,3,4,4a,8a-hexahydronaphthalen-1-yl)pentadecanoate against 2 HsNMT1 protein target, from Leaf Extract of Spondias mombin Linn (SM), has been undertaken to study and characterize two novel ester compounds isolated from leaf extract of SM. Furthermore, anti-Rhino virus properties of the compounds were studied in silico against a known biological target (HsNMT1). This is claimed to be helpful in developing therapeutics against the common cold. It is an interesting subject matter with relation to developing therapeutics against common cold and the study has been meticulously done. It is an original piece of work undertaken by the authors. The experiments undertaken for analyzing data reach to a logical conclusion. The abstract is appropriate and representative of the content. The references are up to date.

My concerns are:

1. Please revise manuscript for English syntax correction.
2. Consider revising the title to make it concise and understandable.
3. Do we need the heading: significance, in the abstract part?
4. For making the study more concrete, at least the in vitro study should be conducted to confirm the anti-Rhino virus activity of the compounds.
5. TLC test does not add much of significance to the manuscript. Please add some reasoning to it and revise.
6. For CR3R4 R3, perhaps structural representation would be better.
7. FTIR and NMR studies may be shifted to main manuscript.
8. What does EIMS stand for and DEPT-35.
9. The control taken is not explained in the initial paras where biological targets are introduced.
10. Explain the activities with regards to biological activity in Table 4.
11. What is significance of the sentence: However, in comparing the relative flexibilities of the simulated systems, the complexed HsNMT1 systems show lower fluctuations in contrast to the native unbound system of HsNMT1, indicating that the bound inhibitors enact rigidity on the protein structure.
12. Check if all Figures are appended where they need to be
13. In Figure S1, replace chromatography with spectroscopy.
14. In Figure S3 and S4, there is so much noise in the data.
15. Figure S13 and Figure S14 are not explained in text.

[See Appendix 1 for Reviewer I's comments made directly on the manuscript]

Author response to Reviewer I: Round 1

The draft: Structures and anti-Rhino virus properties of 6-methylheptyl pentadecanoate and 6-1

methylheptyl 15-(1,2,3,4,4a,8a-hexahydronaphthalen-1-yl)pentadecanoate against 2 HsNMT1 protein target, from Leaf Extract of Spondias mombin Linn (SM), has been undertaken to study and characterize two novel ester compounds isolated from leaf extract of SM. Furthermore, anti-Rhino virus properties of the compounds were studied in silico against a known biological target (HsNMT1). This is claimed to be helpful in developing therapeutics against the common cold. It is an interesting subject matter with relation to developing therapeutics against common cold and the study has been meticulously done. It is an original piece of work undertaken by the authors. The experiments undertaken for analyzing data reach to a logical conclusion. The abstract is appropriate and representative of the content. The references are up to date.

Thank you for the comment.

Please revise manuscript for English syntax correction.

Thank you for your comment: Authors have corrected all English syntax errors.

Consider revising the title to make it concise and understandable.

Thank you for your insightful comment. Thank you for the comment. The title has been revised. "PHARMACO-PHYTOCHEMISTRY OF ESTERS ISOLATED FROM LEAF EXTRACTS OF SPONDIAS MOMBIN AS POTENTIAL ANTIVIRAL AGENT."

Do we need the heading: significance, in the abstract part?

Thank you for your comment. Thank you for the comment. Significance has been deleted.

For making the study more concrete, at least the in vitro study should be conducted to confirm the anti-Rhino virus activity of the compounds.

Thank you for your insightful comment. The authors recommended that further studies such as *in vitro* and *in vivo* studies must be conducted in future investigations.

TLC test does not add much of significance to the manuscript. Please add some reasoning to it and revise.

Thank you for the comment. TLC test was added to the manuscript to give a rationale as to why certain aliquots were bulked up together according to their similar R_f-value (retention factor) SP^3 carbon (C-H stretch), this wavelength being reported by other authors at a figure between 2961 cm^{-1} and 2923 cm^{-1}

For CR3R4 R3, perhaps structural representation would be better.

Thank you for the comment. R3,R4= alkyl,

FTIR and NMR studies may be shifted to main manuscript.

Thank you for the comment. FTIR and NMR studies, make the manuscripts more cumbersome, also guidelines of the journal indicate that they must be in the supplementary/appendix.

What does EIMS stand for and DEPT-35.

Thank you for the comment. Electron Ionization Mass Spectroscopy (EIMS), Distortionless Enhancement by Polarization Transfer (DEPT-135)

The control taken is not explained in the initial paras where biological targets are introduced.

Thank you for the comment.

Explain the activities with regards to biological activity in Table 4.

Thank you for your insightful comment: The biological activity was explained in the first sentence of the paragraph. 'A biological activity spectrum for a substance is a list of biological activity types for which the probability to be revealed (Pa) and the probability not to be revealed (Pi) are calculated. Pa and Pi values are independent and their values vary from 0 to 1. Biological activity spectra were predicted for the two isolated structures of 6-methylheptyl pentadecanoate and 6-methylheptyl-15-(1,2,3,4,4a,8a-hexahydronaphthalen-1-yl)pentadecanoate via PASSonline 2005 version'

What is significance of the sentence: However, in comparing the relative flexibilities of the simulated systems, the complexed HsNMT1 systems show lower fluctuations in contrast to the native unbound system of HsNMT1, indicating that the bound inhibitors enact rigidity on the protein structure.

Thank you for the comment. Sentence revised.

Check if all Figures are appended where they need to be

Thank you for your comment. All Figures have been checked.

In Figure S1, replace chromatography with spectroscopy.

Figure S1: FTIR spectroscopy of CS1

In Figure S3 and S4, there is so much noise in the data.

Thank you for the comment. Authors had to show the entire spectroscopy.

Figure S13 and Figure S14 are not explained in text.

The 2D NMR of proposed compound CS2 demonstrated varying coupling dimension. Typical example is the two protons on carbon 10 close to carbonyl moiety coupled with it adjacent proton on carbon 9 (Fig. 7) as confirmed by HSQC Fig 9. Similarly, proton on carbon 12 and 13 can also be confirmed by the HSQC spectrum which also coupled with each other to give triplet at δ 2.29 and 1.65. The methylene protons between carbon 4 and carbon 8, as well as carbon 14 and 23 shifted up field and overlap at δ 1.261.

Author response: Other additions

The omitted J values were for compound CS2 and not CS1.The corrections made are indicated below and highlighted in red in the corrected version on page 165-166:

"^{1}H NMR (CDCl3 , 400 MHz) δ^{1}**H** (ppm): 7.66 (1H, J =2.4Hz, H-5), 7.12 (1H, d, J =8.8Hz, H-6) , 6.8 (1H, J =8.8Hz, H-7), 4.16(1H, d, J = 3.32 Hz, H-10), 3.97(1H, J=2.32Hz H-4), 3.96(1H, J = 3.42Hz, H-8), 3.63, (1H, d, J =5.92Hz), 3.30, (1H, d, J =5.8Hz), 2.29(1H, d, J = 5.84Hz, H-9), 1.53 (2H, d, J = 3.52 Hz, H-18), 1.26, (25H, m H-19, 20, 22, 25-28), 0.86(10H, m H-24)."

Reviewer E: Round 1

Not openly accessible under our Publishing peer review reports policy.

Structures and anti-Rhino virus properties of 6-methylheptyl pentadecanoate and 6-methylheptyl 15-(1,2,3,4,4a,8a-hexahydronaphthalen-1-yl)pentadecanoate against HsNMT1 protein target, from Leaf Extract of *Spondias mombin Linn*

ABSTRACT

The present work reports on the isolation and characterization of two novel antiviral ester compounds from Dichloromethane leaf extracts of *Spondias mombin (SM)*. The characterization and structural elucidation were established from spectroscopic evidence of NMR, FTIR and mass spectroscopy (MS/MS). The compounds identified were 6-methylheptyl pentadecanoate and 6-methylheptyl-15-(1,2,3,4,4a,8a-hexahydronaphthalen-1-yl)pentadecanoate . The novel isolated ester compounds were reported to have anti-Rhino virus activity *in silico* against a known biological target (HsNMT1) that plays a key role in developing therapeutics against the common cold. Molecular docking analysis revealed the binding affinity across all targets within the range of -4.6 to -8.2kcal/mol, while Molecular Dynamic simulation showed that systems attained good stability due to the maintenance of mean RMSD values within the acceptable range of 1.5 -2.5Å. It can be concluded that the novel compounds are potential inhibitory candidates against Rhinovirus protein target HsNMT1. However, *in vitro* and *in vivo* experiments are further required to validate the possible inhibitory candidates against Rhinovirus disease (common cold).

KEYWORDS: *Spondias mombin*, phytochemistry, ethnomedicine, pharmacological activity, esters, Rhinovirus.

SIGNIFICANCE

The significance of this study contributes to the scientific rationale for the use of *SM* leaf extracts in treating viral diseases Two novel compounds isolated were 6-methylheptyl pentadecanoate and 6-methylheptyl-15-(1,2,3,4,4a,8a-hexahydronaphthalen-1-yl)pentadecanoate were predicted to possess anti-rhinovirus properties, through computer-aided techniques.

INTRODUCTION

Novel phytochemical compounds have diverse phytochemical and pharmacological properties. These phytochemicals are abundant in natural products(1), with some used as new drugs leading to drug discovery(2). The combination of ethnomedicinal uses, phytochemistry and pharmacological properties of crude, fractionated and /or isolated, pure compounds against numerous biological targets have led to the discovery of numerous drugs in the treatment of infectious diseases(3-5). Natural products such as *Spondias mombin* (*SM*)(Anacardiaceae) leaf extracts have been used to treat several infectious diseases (6). The pharmacological activities of leaf extracts of *S. mombin* (*SM*) have been attributed to some bioactive compounds isolated from the medicinal plant. Some of these isolated compounds from leaf extracts of *S. mombin* include esters such as 3β-Olean-12-en-3-yl (9Z)-hexadec-9-enoate(7), chlorogenic acid butyl ester(8) and caffeoyl ester (9, 10). The leafs are reported to be part of the medicinal plant mostly used for treating viral respiratory infections such as rhinovirus in traditional African healing systems (11).

Human Rhinoviruses affect the upper and lower respiratory tract and cause common colds associated with pneumonia, wheezing and asthma (12).

Isolated compounds from natural products are identified by several chromatographic and spectroscopic methods such as Thin Layer Chromatography (TLC), Column Chromatography(CC), Fourier Transform Infrared (FTIR) Spectroscopy, Gas chromatography and Mass spectroscopy (GC-MS) and Nuclear magnetic resonance (NMR) among others. These methods for separation, Identification and structural determination of phytochemicals are becoming increasingly powerful(13). TLC might be the simplest of all chromatographic methods, but it provides critical information in identifying compounds separated by other methods during the phytochemistry analysis of natural products (14).

FTIR is known to identify only the types of functional groups in a compound, most commonly, CH_2, CH_3, = CH, ≡CH, O-H, C = O, C-O, C = C, C≡C, C-O-C and C-C- O (15). FTIR and NMR analysis, coupled with mass spectroscopy (MS), are helpful tools in the structural elucidation of an isolated compound.

In other to assess the therapeutic potential of the selected compounds via *in silico* methods, it was necessary to identify a peculiar biological target. The prediction of biological activities of the compounds was determined by utilizing the PASSonline software(16). This software is utilized for the prediction of different physiological activities for multiple compounds, both natural and synthetic, based on their chemical formula. Additionally, PASS Online predicts also pharmacological effects, mechanisms of action, adverse effects, interaction with metabolic

enzymes and transporters, and influence on gene expression. It uses the 2D molecular fragments known as multilevel neighbors of atoms descriptors, which postulates that a compound's molecular structure determines how active it is biologically(17). With this software, the evaluated activity of a compound is estimated as probable activity (Pa) and probable inactivity (Pi)(18).

The current study aims to isolate, identify, characterise and predict antiviral properties through Molecular Targets prediction of novel compounds from Dichloromethane (DCM) leaf extracts of *SM*. The study revealed, for the first time, two ester compounds from *SM* leaf extract that possess antiviral properties in an *in silico* molecular target prediction.

METHODS

Material processing and extraction

Fresh leaves of *SM Linn* were collected from Cape Coast - Ghana and authenticated by Mr. [anonymised] at the Herbarium section of the University of [anonymised] and given a voucher number [anonymised]. Leafs dried at room temperature were pulverized by using a hammer mill. The leaf powder of mass 100 g was initially defatted with 1 L of hexane and then extracted with 2 L DCM by cold maceration for 72 h until the solvent was clear. The extracts were filtered with filter paper and concentrated using a rotary evaporator under reduced pressure at 40˚C. The concentrate was completely dried with a weight of 5.19g (5.17%) and denoted as SMDCM.

General Analytical Information.

^{1}H and ^{13}C NMR spectra were recorded on Bruker AV 400 MHz instrument at 400 MHz (1H NMR) and 100 MHz (^{13}C NMR). All ^{1}H NMR spectra were measured in parts per million (ppm) downfield or relative to the residual proton signals of d1-chloroform ($CDCl_3$,7.26ppm). All ^{13}C NMR spectra were reported in ppm relative to residual carbon signals of $CDCl_3$ (77.16 ppm). Coupling constants (J) are reported in hertz (Hz). Multiplicity is indicated as follows: s (singlet), d (doublet), t (triplet), q (quartet), p (pentet), and m (multiplet) (15). Thin-layer chromatography (TLC) was performed on precoated Merck Silica gel 60 F254 plates using different polarities of hexane-ethyl acetate solvent systems and compounds were visualized with UV light at 254 nm(19). The R_f values of the different spots that were observed were calculated (20).

The retention factor (R_f) values were calculated using the equation below:

$$R_f = \frac{Distance\ traveled\ by\ the\ solute}{Distance\ traveled\ by\ the\ solvent}$$

FTIR Spectroscopy was performed using PerkinElmer Spectrum 100 spectrophotometer at room temperature, while MS of isolates was determined by using CombiFlash Purlon Mass Spectrometer (2000 Da Polarity Auto Switching).

Preliminary Phytochemical screening of SMDCM extract

Preliminary phytochemical screening was performed as a qualitative process to investigate the presence of different classes of phytochemicals according to standard procedures as reported by other authors (21, 22). Briefly, crude DCM leaf extract of *SM* was used for the qualitative analysis to determine the presence of alkaloids, steroid flavonoids, saponins, terpenoid tannins, anthraquinone derivatives, and cardiac glycosides.

Column fractionation of SMDCM mixture

The *SM* DCM extract was loaded onto a glass column packed with silica gel. It was then eluted with mixtures of ethyl acetate and hexane of increasing gradient polarity, starting with 100% hexane to 100% ethyl acetate. One hundred and seventy-one fractions were collected in 50 mL aliquots and based on their TLC analysis, aliquots 55 to 100 were bulked together (denoted C) for further separation of the two compounds. It was further separated using column chromatography with silica gel using a solvent mixture of gradient, ethyl acetate and hexane. Seventy fractions were collected in 10 mL aliquots and based on the TLC, aliquots 1 to 23 were bulked into CS1 and 24 to 70 into CS2.

Characterization of Isolated Compounds

Chemical shifts are reported about DSS-trimethyl singlet resonance at 0.0000 ppm and multiplicity.

Characterization of CS1

A dark green solid, CS1: FTIR (KBr) vmax cm^{-1}: 2927 (CH_2), 1748(C=O), 1465 (CH bending), 1220 (C-O), 725(CH). ^{1}H NMR ($CDCl_3$, 400 MHz) δ**^{1}H** (ppm): 3.96(2H, q, J = 2.56 Hz, H-8), 2.30 (2H, q, J = 4.72 Hz, H-10), 1.64(1H, m, H-11), 1.55 (1H, q, J = 5.96 Hz, H-2), 1.30 (30H, m, H4-7, H-11-21) 0.90 (12H, m, H1&3, H23&22). ^{13}C NMR ($CDCl_3$, 400 MHz) δ^{13}C (ppm): 173.57(C-11), 79(C-10), 68(C-9),40 (C-8), 36 (C-7), 35(C-6), 32(C-5), 30(C-4), 22-25(C-3), 14.03-14.11 (C-2),10.97 (C-1).

Characterization of CS2

A dark green solid, CS2: FTIR (KBr) νmax cm^{-1}: 2927 (CH_2),1748(C=O), 1465 (C-H bending), 1220 (C-O), 725(C-H). ^{1}H NMR (CDCl3 , 400 MHz) δ^{1}**H** (ppm): 7.66 (1H, d, J = Hz, H-5), 7.29 (1H, d, J = Hz, H-6) , 6.64 (1H, d, J = Hz, H-7), 3.96(2H, q, J = 2.48Hz, H-8), 2.300(2H, d, J = 5.84 Hz, H-10), 1.64(2H, m, H-4), 2.68(1H, d, J = Hz, H-9), 1.63,1.38 (H, d, J = Hz,), 1.54 (1H, d, J = Hz, H-23), 1.53 (2H, d, J = 3.52 Hz, H-18), 1.26, (25H, tm H-19, 20, 22, 25-28), , 0.86(10H, m H-24).13C NMR ($CDCl_3$, 400 MHz) δ^{13}C (ppm): 173.57 (C-9), 127.58 (C- 33), 114.03(C-30), 66.81(C-8), 38.74(C-18), 34.00(C-17), 31.93(C-16), 30.41(C-15), 29.70(C-14), 29.66(C-13), 29.36(C-12), 28.92(C-11), 24.48(C-7), 23.79(C-6), 22.96(C-5), 22.69(C-4), 14.11(C-3), 14.04(C-2), 10.98(C- 1) .

Biological Activity Prediction via PASSonline

PASSonline software(16) is used to predict physiological activities, pharmacological effects, mechanisms of action, toxic and adverse effects, interaction with metabolic enzymes and transporters and influence on gene expression for multiple compounds, both from natural products and synthetic, based on their chemical formula.

The evaluated activity of a compound is estimated as probable activity (Pa) and probable inactivity (Pi)(18). Compounds presenting Pa higher than Pi relative to a particular activity are considered feasible for that specific medical activity and those with Pi higher than Pa were therefore eliminated. To this end, the selected compounds were assessed for their biological activities on PASSonline.

Molecular Docking

The X-ray crystal structures of some selected rhinovirus antiviral targets (PDB ID: 5FX6, 5MU6, 4C2X and 1CQQ (23)were retrieved from the Protein Data Bank(24). These structures were co-crystallized with native inhibitors that defined their respective binding site. The structures, 5FX6, 5MU6, 4C2X and 1CQQ, were then prepared by using UCSF Chimera version 1.13.1(25) to remove all non-standard residues and Modeller 9.25 version (26) was employed to fix missing residues. The binding site residues were obtained by zoning the native inhibitors and selecting residues that lie within 5Å for each target protein. Subsequently, the isolated compounds were optimized using Avogadro 2.0 software and saved. Molecular docking was carried out for the three selected compounds against each of the rhinovirus target

proteins using Prix software. The target which showed the best docking property against all compounds was selected for molecular dynamics simulation.

Molecular Dynamic simulation(MD)

MD simulations were performed using the AMBER18 GPU package for the best-docked ligand; CS1 and CS2 and IMP-1088 to the target (HsNMT1). The ligand and receptor were both defined and optimized using the AMBER force fields by using the Antechamber and LEAP modules, respectively. Solvation and neutralization were carried out for the receptor prior to its combination with the ligand. Partial minimization of the receptor in the system was conducted for 2500 steps with a restraint potential of 500 kcal/mol Å2, followed by complete minimization of 10 000. The system underwent heating at 300K using Langevin thermostat in a canonical ensemble (NVT). Equilibration of the system was carried out to ensure that AMBER rechecks the system and it was at 300K. MD simulation was run for 12 hrs. at 100ns, and results were obtained in the form of trajectories and analysed using statistics. The trajectories generated allow for the measurement of the binding energies of the association of the ligand to the receptor. Visualization of the interactions was produced from Snapshots and Discovery studio.

Binding Free Energy Analysis via MM/GBSA Method

The Molecular Mechanics/Generalized Born Surface Area (MM/GBSA)(27, 28) method was employed in estimating the binding free energy for each of the inhibitor-bound systems. The binding free energy **(ΔG_{bind})** was calculated from the following equation:

$\Delta G_{bind} = G_{complex} - G_{receptor} - G_{ligand}$ (1)

$\Delta G_{bind} = E_{gas} + \Delta G_{sol} - TS,$ (2)

Where ΔG_{bind} is considered to be the summation of the gas phase and solvation energy terms less the entropy (TS) term

$E_{gas} = E_{int} + E_{vdw} + E_{lec}$ (3)

E_{gas} is the sum of the AMBER force field internal energy terms E_{int} (bond, angle and torsion), the covalent van der Waals (E_{vdw}) and the non-bonded electrostatic energy component (E_{lec}). The solvation energy is calculated from the following equation:

$G_{sol} = G_{GB} + G_{non\text{-}polar}$ (4)

$G_{non\_polar} = \gamma SASA + b$ (5)

Where ΔG_{bind} is taken to be the sum of the gas phase and solvation energy terms less the entropy ($T\Delta S$) term., $_{Complex}$ represents the energy of the receptor-ligand complex. Whiles

$G_{receptor}$ and G_{ligand} represent energies of receptor and ligand, respectively. Egas denotes gas-phase energy; Eint signifies internal energy; and E_{ele} and E_{vdw} indicate the electrostatic and Van der Waals contributions, respectively. E_{gas} is the gas phase, elevated directly from the FF14SB force terms. G_{asol} denotes solvation-free energy and can be decomposed into polar and nonpolar contribution states. The polar solvation contribution, G_{GB}, is determined by solving the GB equation, whereas G_{SA}, the nonpolar solvation contribution, is estimated from the solvent accessible surface area (SASA) determined using a water probe radius of 1.4 Å. T and S correspond to temperature and total solute entropy, respectively. Γ Is a constant(29). Per-residue decomposition analyses were also carried out to estimate the individual energy contribution of residues of the substrate pocket towards the affinity and stabilization of each target

RESULTS AND DISCUSSION

Figures 1 and 3 show structures of isolated esters: 6-methylheptyl pentadecanoate and 6-methylheptyl 15-(1,2,3,4,4a,8a-hexahydronaphthalen-1-yl)pentadecanoate from DCM leaf extracts of *SM*. The FTIR, NMR and MS/MS spectra of the isolated compounds are provided in the supplementary materials (**Figures S1- S14**)

Preliminary Phytochemical screening and TLC test of compounds CS1 and CS2

Table 1 indicates a phytochemical test to examine the qualitative chemical constituents contained in leaf extracts of *SM*. The phytochemical test revealed the presence of anthraquinone derivatives, steroids, tannins and cardiac glucosides. The results of the preliminary phytochemical screening are in line with reports by other authors (30, 31).

The percentage yield in this study was calculated using the weight of extracted sample divided by the total sample used and found to be 11.14% (**Table 2).**

During the TLC test, the retention factor values obtained in this experiment (**Table 3**) did not give many clues as to the type of compounds in the extract, but they suggest the polarity of the compounds as reported by Talukdar *et al.*(2010) (14). The authors indicated that a high R_f value in a less polar solvent system possesses low polarity (14).

Table 1: Preliminary Phytochemical screening of SMDCM extract

Class of phytochemicals	Tests performed	*Spondias mombin* leaf extracts
		SM-DCM
Alkaloids	Meyer	-
Anthraquinones Derivatives	Bontrager test	+
Steroids	Liebermann-Burchard test	+
Terpenoids	Liebermann-Burchard test	-
Saponins	Frothing	-
Flavonoids	Sulfuric acid test	-
Tannins	Ferric chloride test	+
Cardiac glucosides	Keller Killian	+

Key: + present, - absent

Table 2: Physical properties and percentage (%) yield from 60g SMDCM dry powder.

Physical properties	**SM-DCM leaf Extract**
Physical appearance	Yellowish green
Yield/ Weight of crude extract (g)	6.688g
% Yield	11.14%

Table 3: TLC test of CS1 and CS2

S.No.	**Solvent phase**	**Distance traveled by solvent (cm)**	**Distance traveled by the solute (cm)**	**Experimental RF Values**	**RF Values literature**	**Color of Peaks**
CS1	30 % v/v hexane in ethyl acetate	2.8	2.0	0.714	0.71 (Phenolics) (32-35)	dark
CS2	30 % v/v hexane in ethyl acetate	2.8	1.3	0.464	-	dark

Structural elucidation of CS1

The FTIR spectrum was used to identify the functional groups of the active components present in the extract based on the peak values in the region of IR radiation. When the extract was analysed by FTIR, the functional groups of the components were separated based on their peak ratio.

The peak values were recorded in **Table TS1** and **Figure S1** for CS1, indicating the carbonyl group, which represents an ester with C=O stretch, was observed at 1748.0 cm^{-1} with very strong intensity (1750 -1735cm^{-1}) (36). This is in line with the reported carbonyl group 1750cm^{-1} by Wang, *et al.*, (2019) (36). At 1748.0 cm^{-1}, the peak assigned to C=O ester was confirmed by other researchers to be between 1734–1745 cm^{-1} (37-39). An aliphatic ester O=C-O-C, with

two bands, one stronger than the other, was also observed at 1220.0 cm^{-1} (1160-1210 cm^{-1}) (40, 41). As noted, the two bands at 1220.0 cm^{-1}, with one stronger than the other, attributed to the presence of an aliphatic ester C-O, although Jain *et al*., 2016 (42) assigned a C-O stretching at 1253.97 cm^{-1} and 1054.89 cm^{-1}. Compound CS1 has bands at 2927.0 cm^{-1} that are due to the symmetric stretching of the S_P^3 carbon (C-H stretch), this wavelength being reported by other authors at a figure between 2961 cm^{-1} and 2923 cm^{-1} (39, 42-44). Findings from this study revealed a band at 1465.0 cm^{-1}, indicating a C-H bending, although other investigators reported the C-H bending at 1470cm^{-1} (44).

The NMR analysis of CS1, referenced with **Table TS2**, indicates that the proton shifts between carbons C1-C7 are aliphatic alkanes, with carbons C8, C10, C11 and C2 at 3.96ppm (q,2H,J=2.59Hz, H-8)(45), 2.30 ppm (q, 2H,J=4.72 Hz,H-10) (6, 46, 47), 1.64 ppm (m, 1H,H-11) (48), 1.55 (1H, q, J = 5.96 Hz, H-2), with, 0.9 ppm (m, 12H, H1&3, H23&22) (48-51). Carbon C8 is an alkyl (-CH_2) of the ester, with C10 showing a carbonyl ester group (O-CH_2); this is in line with the literature and reported to be an alkyl adjacent to a heteroatom (R-O-CH_2)(36, 48, 52). Proton on carbon C10, indicated two Hydrogen quartets at 2.30ppm, which is in line with reports by Buckingham, A. D. (1960) (48), who also revealed a band at 2.30ppm to be CH_3COR (48). The singlet hydrogen, occurring at 7.25ppm (7.05 - 7.25ppm), indicates a proposed functional group of CR^3R^4 R^3 (48).

Table TS4 indicates the analysis of ^{13}C NMR spectrum for CS1, which revealed that the ^{13}C spectrum has approximately 16 carbon peaks (δ 10.97, 14.03-14.11, 22-25, 30, 32, 35, 36, 40, 68, 79 and 173.57 ppm), as expected given the top/bottom overlaps in the spectrum, with a strong carbonyl peak at 173.57ppm assigned to carbon 9 (**Figure 1**).

The DEPT-135 obviously distinguishes between the methyl (–CH_3) (14.11, 14.04 and 10.97 ppm), methine (CH) (38.74ppm) and methylene (52)(–CH_2) (66.63, 34.01, 31.93, 30.41, 29.70, 29.37, 28.92, 24.49, 23.79, 22.99, 22.69 ppm)(52, 53) of the ethyl chain (**Figure S7 and S12**). The peak, close to carbonyl at 66.63 ppm, was assigned to -CH_2- carbon 8, that of tertiary carbon two at 34.01 ppm, while primary carbons 1 and 3 also appeared at 14.11 ppm and 14.04 ppm, respectively. The rest of the methylene carbons 4-7 could be seen at 29.37- 31.93 ppm **(Figure 4).**

EIMS of the isolated compound CS1 showed a mass ion peak at m/z 355 [M+H] (**Figure S3**), from which a molecular formula of $C_{23}H_{46}O_2$ was assigned. Typically, molecule CS1, at a retention time (Rt) of 0.714 min (**Table 3**), produced a precursor ion at m/z 355 [M+H], and the fragmentation of this molecule (**Figure 2**) generated product ions at m/z 298. These were derived from the loss of the isobutyl side chain (-57 Da) after a possible 1,3 methyl

rearrangement of isopropyl derivative of methyl heptyl pentadecanoate to a more stable butyl pentadecanoate derivative (**Figure 2**). Products ions at m/z 284, due to the neutral loss of methyl (−14 Da), and at m/z 266 (loss of propyl molecule) were also observed. Based on these data, CS1 was identified as 6-methylheptyl pentadecanoate.

Authors, therefore, propose the structure and IUPAC name for compound CS1 based on the information obtained as 6-methylheptyl pentadecanoate.

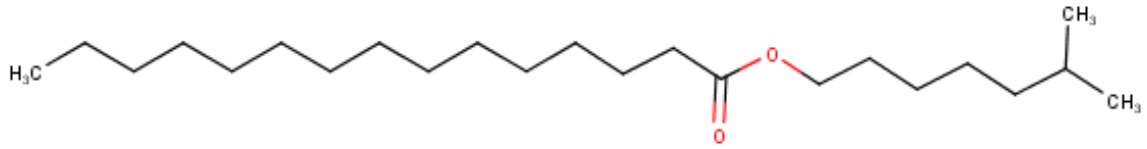

Figure 1: Proposed structure of CS1

The fragmentation pattern of 6-methylheptyl pentadecanoate was based on the analysis of mass spectroscopy **in Figure S3.** The fragmentation pattern is indicated below (**Figure 2).**

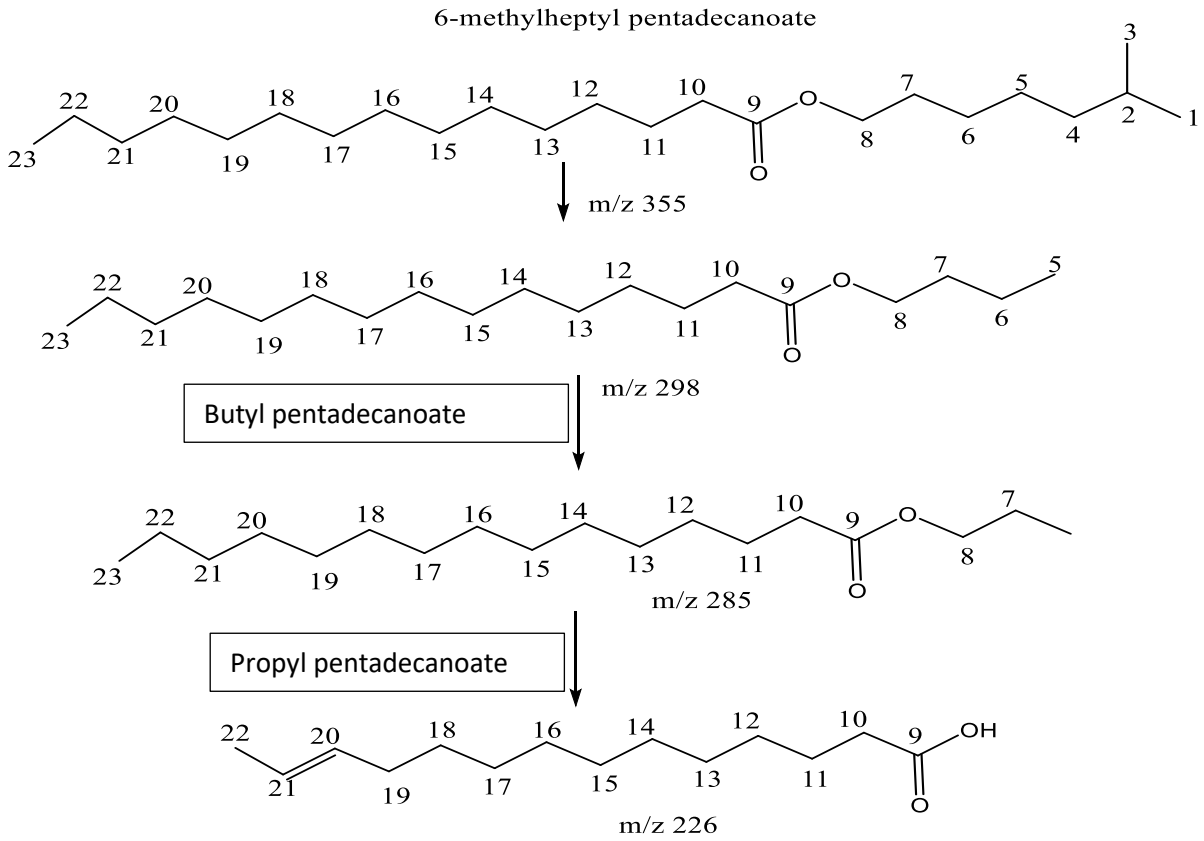

Figure 2: Fragmentation pattern of CS1 from the mass spectroscopy.

Structural elucidation of CS2

Similar to the FTIR analysis of **Table TS1 and Figure S2**, compound CS2 indicates that the isolated compound is an ester. Evidence of the presence of an ester showed peaks at 1748 cm^{-1} and 1220 cm^{-1}, indicating the functional groups of C=O and C-O, respectively(36, 40, 41). The NMR data analysis, as indicated in **Table TS3**, revealed that compound CS2 showed proton shifts on carbons C10-C17 as aliphatic alkanes, $-CH_2-CH_2$ between 1.19- 1.26ppm (0.8-1.6ppm) (45, 46). Protons on carbon numbers C18 – C23 and C25 - C28 indicate the presence of Cyclic alkane, CH_2-CH_2-CH with shifts between 1.20- 1.63ppm (1.2-1.7ppm)(6, 45, 46). Similarly, proton shifts of carbons 5-8, between 5.80 and 7.29 ppm (4.0-7.3ppm), indicate an alkene, HC=CH (54, 55). A proton shift of 7.66ppm on carbon 5, =CH, shows that the compound CS2 contains a Cyclic alkene(54). Significantly, on compound CS2, the proton on carbon number 8 indicated an alkyl of ester, $-OCH_2$ at 4.20ppm (3.5-4.8ppm), while proton adjacent to C=O on carbon 10, 2.88ppm (2.0-3.0ppm), shows –CH. Proton on carbons C8 confirms the ester nature of CS2 (54, 55). **Table TS5** indicates the analysis of ^{13}C NMR spectrum, with approximately 19 carbon peaks (δ 10.98, 14.04, 14.11, 22.69, 22.96, 23.79, 24.48, 28.92, 29.37, 29.66, 29.70, 30.41, 31.93, 34.00, 38.74, 66.81 114.03, 127.58 and 173.57 ppm), as expected given the overlaps in the spectrum, with a strong carbonyl peak at 173.57ppm, assigned to carbon 9 (**Figure 3**).

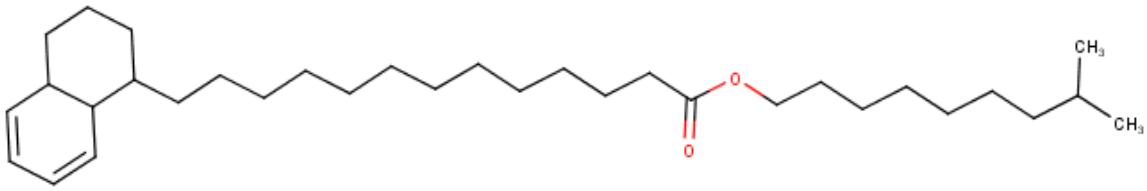

Figure 3: Proposed structure of CS2

The mass spectrometric analysis of CS2**,** showed a mass ion peak at m/z 489 (M+H) from which a molecular formula of $C_{33}H_{60}O_2$ was assigned (**Figure S4**). A retention time of (Rt) of 0.464 min (**Table 3**) produced a precursor ion at m/z 489 [M+H] and fragmentation of this molecule (**Figure 7**) generated product ions at m/z 414, derived from the loss of isopentyl side chain (-75 Da), m/z 359 due to loss of propanol (-58 Da), m/z 300 also due to loss of the second propanol (-59 Da). Based on these data, in addition to the NMR and FTIR data, molecule CS2 was identified as 6-methylheptyl-15-(1,2,3,4,4a,8a-hexahydronaphthalen-1-yl)pentadecanoate. The fragmentation pattern of CS2 was based on the analysis of mass spectroscopy **of Figure S4.** The fragmentation pattern is indicated below (**Figure 4).**

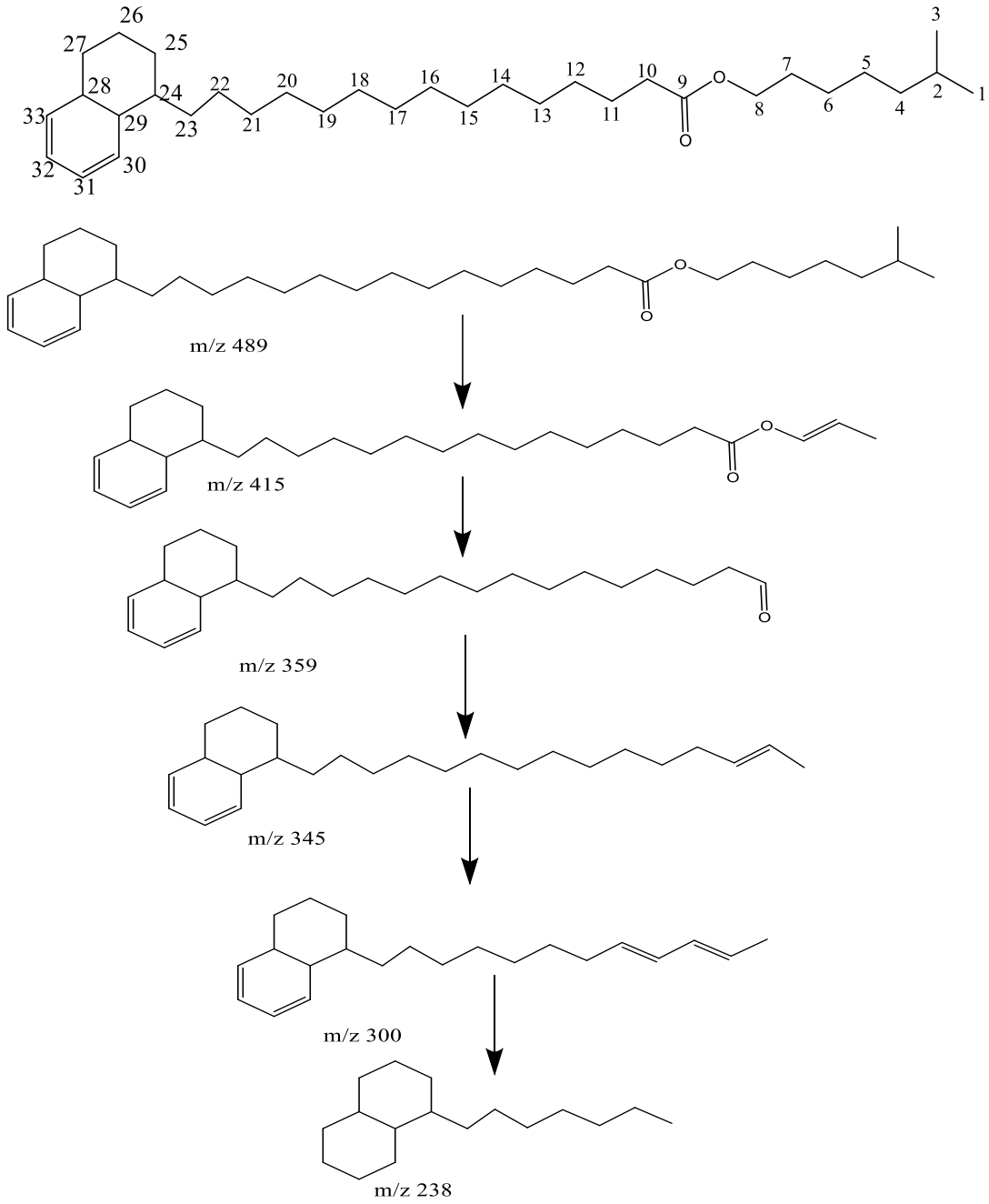

Figure 4: Fragmentation pattern of CS2 from the mass spectroscopy.

Biological Activity prediction

A biological activity spectrum for a substance is a list of biological activity types for which the probability to be revealed (Pa) and the probability not to be revealed (Pi) are calculated. Pa and Pi values are independent and their values vary from 0 to 1. Biological activity spectra were predicted for the two isolated structures of CS1 and CS2 via PASSonline 2005 version (56). Generally, in predicting the desired biological activity, Pa>Pi is considered feasible since there is a high chance of the compound revealing that particular activity. If Pa>0.7, the compound is likely to reveal its activity in experiments, but in this case, the chance of being

the analog of the known pharmaceutical agent is high. If 0.5<Pa<0.7, the compound is likely to reveal this activity in experiments, but this is less and the compound is not so similar to the known pharmaceutical agent. If Pa <0.5, the compound is unlikely to reveal this activity in experiments, but if the presence of this activity is confirmed in the experiment, the compound might be a new chemical entity. The biological activities predicted for each of the compounds herein include antieczematic, phobic disorders, and antipruritic for CS1, as shown in **Table 4**. Whilst antieczematic, antiulcerative and antieczematic, were predicted for CS2 also shown in **Table 1.** Findings from the biological activity prediction show that all two compounds had diverse activities towards different biological processes. However, the selected compounds were predicted to have a common antiviral property, particularly against rhinovirus.

In this study, special attention was given to certain reported activities of *SM* to actively have antiviral properties (57, 58). Hence the selection of a suitable biological activity related to the antiviral activity for its isolated compounds CS1 and CS2 was feasible. Additionally, the desired novelty of a chemical compound is important as well. The predicted Pa values for CS1 (0.655) and CS2 (0.643) both correlated to antiviral activity (Rhinovirus) which falls within the 0.5<Pa<0.7 thresholds correlating to a novel compound that has no known similarity to a known pharmaceutical agent. Subsequently, various antiviral macromolecules were selected to test the efficiency of CS1 and CS2 via *in silico* molecular docking.

Table 4: Predicted biological activity via PASSonline.

Biological Activity					
CS1			CS2		
Pa	**Pi**	**Activity**	**Pa**	**Pi**	**Activity**
0.962	0.002	Eye Irritation	0.868	0.012	Phobic disorders
0.944	0.003	Phobic disorders	0.757	0.005	Cholesterol antagonist
0.820	0.015	Antieczematic	0.723	0.030	Antieczematic
0.713	0.007	Antipruritic	0.730	0.005	Antiulcerative
0.655	0.004	**Antiviral(Rhinovirus)**	0.643	0.013	**Antiviral(Rhinovirus)**

Key: Pa= probability to be revealed Pi = probability not to be revealed

Molecular docking

Molecular docking of selected Rhinovirus targets was, Human rhinovirus HRV (5FX6), HsNMT1 (5MU6), HsNMT2 (4C2X), and Rhinovirus 3C protease (1CQQ). The compounds showed to have good binding towards the selected targets, as evidenced by obtaining an overall binding affinity in the range -4.6 to -8.2kcal/mol across all targets, as shown in **Table 5.** However, CS1 and CS2 proved to have the best binding affinity when docked to HsNMT1 (5MU6), suggesting they may have a potential activity towards HsMNT1 macromolecule which is an attractive target in developing therapeutics against the common cold.

Table 5: Molecular docking Scores

Compound	Binding energy Kcal/mol			
	HRV(5fx6)	HsNMT1 (5mu6)	HsNMT2(4c2x)	HRV 3C(1CQQ)
CS1	-4.6	**-7.6**	-7.3	6.5
CS2	-4.2	**-8.2**	-7.9	7.0
Rupintrivir(reference)	-7.7	X	X	X
imp-1088(reference)	X	-11	-9.8	X
AG7088(reference)	X	X	X	6.5

Analysis of Molecular Dynamic simulation

Molecular dynamic simulations were conducted to assess the conformation dynamics as well as the spatial distribution of atoms in the backbone structure of HsMNT1upon binding of the compounds. MD simulations were also employed to further validate findings from molecular docking by showing the most stable conformations of the complexed structures across time. Post-MD analyses protocols, including; Root-mean-square deviation (RMSD), and Root-mean-square fluctuation (RMSF), Radius of gyration (RoG), and Solvent accessible surface area (SASA), were employed to provide insights on the structural impact of the phytochemical compounds on HsNMT1. An error assessment was also established in analyzing all MD trajectories to consider technical and biological variability. Eliminating these systematic errors lowers experimental variability and makes it possible to determine the underlying dynamics of protein motions in cellular signaling with greater accuracy.

Structural Stability of HsNMT1

A 150ns MD simulation trajectory was established to analyse the conformational dynamics of the c-α atoms in the backbone structure of HsNMT1 in all the simulated systems. The root means square deviation gives an estimation of the protein convergence and stability of the simulated systems. Furthermore, the RMSD value estimates the average variation in atomic displacement over a given period of time compared to a reference time (59). The acceptable threshold for an average change in RMSD of a protein-ligand complex is between 1-3Å. If the RMSD average is more significant than this threshold, it implies there is an extensive conformational alteration in the structure of the protein. Findings show that systems converged early during the simulation and maintained steady atomic motions till the 150ns simulation run, as shown in **Figure 5A**. The mean RMSD estimated for all the simulated systems were 1.88Å, 2.15Å, 1.54Å and 1.83Å for the unbound HsNMT1, CS1, CS2 and IMP-1088 complex systems respectively. As observed from the findings, all systems attained good stability due to the maintenance of mean RMSD values within the acceptable range of 1.5 -2.5Å during the simulation. Also, good stability highlights the reliability of the simulated systems for further conformational analysis.

Structural Flexibility of HsNMT1

The root means square fluctuations were assessed to determine the relative flexibility of the c-α atoms in the backbone structure of HsNMT1 upon binding of the inhibitors. As such, the RMSF values of the unbound HsNMT1, CS1, CS2 and IMP-1088 in complex with HsNMT1 were estimated to observe the change in protein structural flexibility during the simulation run. As shown in **Figure 5B**, all the selected compounds, including the reference IMP-1088 compound, show a peak area of the protein at Glu130, Leu175, Lys240, Ser315 and Thr395 residual positions that fluctuate the most during the simulation. It was observed that the amino acid residues where the reference IMP-1088 bound have similar structural behavior as that of the phytochemical bound systems of HsMNT1. The mean RMSF values estimated were 0.98±0.03Å, 1.01±0.04Å, 0.87±0.02Å, 0.95±0.03Å for unbound HsNMT1, CS1, CS2 and IMP-1088, respectively, showing that the values are very close to each other. However, in comparing the relative flexibilities of the simulated systems, the complexed HsNMT1 systems show lower fluctuations in contrast to the native unbound system of HsNMT1, indicating that the bound inhibitors enact rigidity on the protein structure.

Radius of Gyration

The spatial arrangement of atoms in a protein-ligand complex system around its axis is known as the radius of gyration (RoG) (56, 60). Estimating RoG is one of the most crucial indicators for predicting a macromolecule's structural activity, and it provides insights into variations in the compactness of the protein complex. Therefore, the stability of the unbound HsNMT1, CS1, CS2 and IMP-1088 complex was estimated by measuring RoG over the 150ns simulation as shown in **Figure 5C**. The respective RoG averages computed were 21.85Å, 21.75Å, 21.77Å, and 21.78Å for the Apo (HsNMT1), CS1, CS2 and IMP-1088 systems. The similarity in mean values of the native unbound state (apo) of HsNMT1 and the bound complexes indicates that the selected compounds do not induce major conformational changes to the active site upon binding.

Solvent Accessible surface area

Solvent-accessible surface area (SASA) impacts the structure and activity of biological macromolecules. SASA analysis provides important insights into residual exposure to surrounding solvent molecules during the simulation. Furthermore, due to the location of active site residues at the surface of the protein, greater insight into residue accessibility to solvent would be important in understanding solvent-like behaviour (hydrophilic or hydrophobic) of a molecule as well protein-ligand complex (61, 62). SASA analysis can also

be used to describe protein folding and unfolding (61). As such, the SASA for the simulated systems was computed, as shown in **Figure 5D**. The averages estimated for the simulated systems were 18570.40Å^2, 17877.74Å^2, 17707.02Å^2 and 18000.32Å^2 for the Apo, CS1, CS2 and Imp-1088 respectively. The SASA values of the complexed systems were slightly lower than the unbound HsNMT1 system, indicating a lower surface area exposed to solvent. The binding of the inhibitors induces rigidity to the amino acids in the structure of HsNMT1 upon binding. Findings further highlight the similarity in the structural impact of the compounds and the reference inhibitor of HsNMT1.

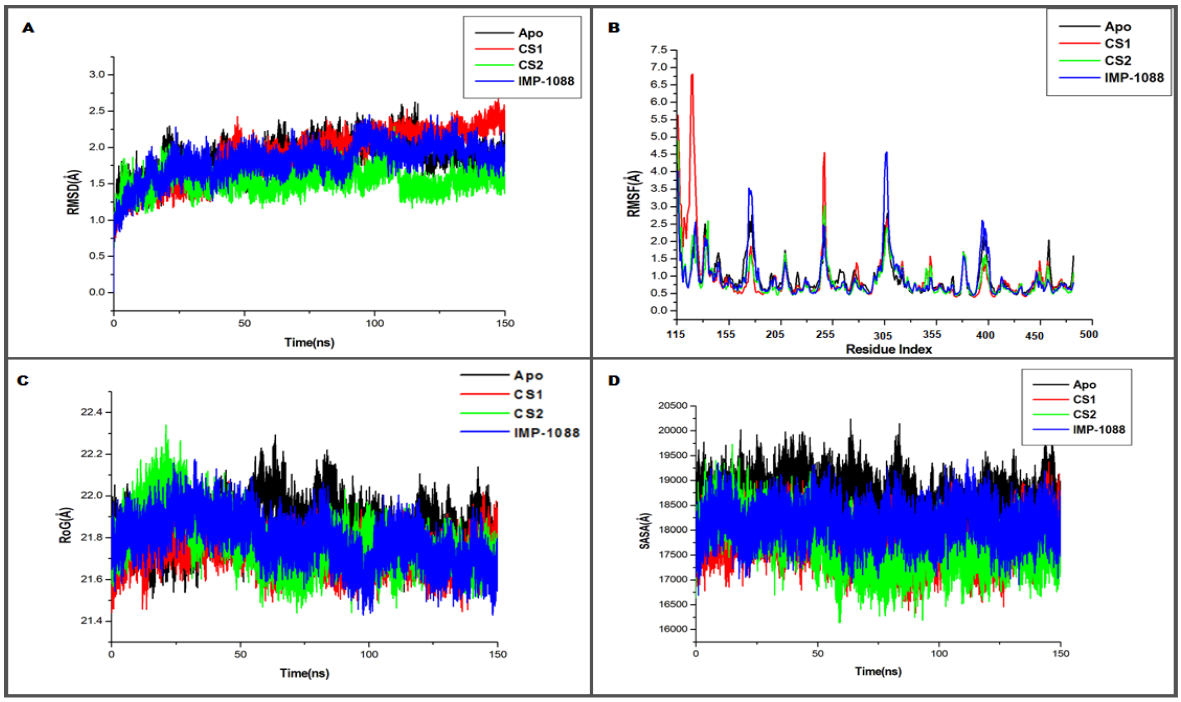

Figure 5: Comparative C-α RMSD, RMSF, RoG and SASA plots showing conformational alterations upon binding of the compounds and reference compound to HsNMT1 over the 150ns MD simulation time **[A]**. Shows the RMSD plots, which indicate the compounds induced relative stability on the HsNMT1enzyme upon binding. **[B]**. Shows the RMSF plots indicating peak regions of residual fluctuations **[C]** Show relative compactness of all simulated systems of complexed structures and the unbound (Apo) system. **[D]** Showing the surface area exposed to solvent between the simulated systems.

Binding Free Energy

The mechanics/generalized-born surface area (MM/GBSA) method was employed to estimate the binding free energetics of the complexed systems of CS1 and CS2 including the reference IMP-1088 compound. It is well recognized that the MM/GBSA method for predicting binding energy is more accurate than the majority of molecular docking scoring

functions and computationally less complex than alchemical free energy techniques (63-66). The computed binding free energies for the complexed systems of HsNMT1 were estimated to be -35.20kcal/mol, for CS1, -44.55kcal/mol for CS2 and -47.06kcal/mol for IMP-1088. Findings show that CS2 had the strongest binding free energy among the two compounds; however, both compounds demonstrated overall stronger energies than the reference compound used in the study. The results indicate that these compounds can be considered potential inhibitors of HsNMT1. **Table 6** indicates the energy terms that contribute to the binding free energy, the most favourable components being the ΔE_{ele}, ΔE_{vdw} and ΔG_{gas}, while $\mathbf{\Delta G_{sol}}$ is unfavourable. The MM/GBSA method is a well-known technique that demonstrates computational effectiveness using implicit solvent and also offers a transparent environment for determining the physical causes of observed effects in protein-ligand interactions (28, 66). Taken together, the energies presented by these compounds suggest the spontaneity, permeation and a measure of the reaction kinetics that characterize their complexing with the target protein.

TABLE 6: Binding free energy estimations via MM/GBSA

Complexes	ΔE_{vdw}	ΔE_{ele}	ΔG_{gas}	ΔG_{sol}	ΔG_{bind}
HsNMT1-IMP-1088	-44.97 ±0.33	-47.24±0.39	-82.21±0.27	54.03±0.36	-35.20±0.15
HsNMT1-CS1	-53.60± 0.23	-10.67 ±0.18	-64.27±0.30	19.72±0.13	-44.55±0.24
HsNMT1-CS2	-60.19±0.32	-5.28±0.29	-65.45±0.43	18.41±0.24	-47.06±0.28

ΔEele = electrostatic energy; ΔEvdW = van der Waals energy; ΔGbind = total binding free energy; ΔGsol = solvation free energy ΔG = gas phase free energy

Binding Interactions

The types of interactions a molecule has in a target protein's binding pocket emphasize how therapeutically effective it is for the protein (67). The binding interactions of CS1, CS2 and the reference IMP-1088 compound bounded to HsNMT1 was assessed. The CS1 and CS2 as potential inhibitors were observed to engage in a variety of interactions involving conventional and carbon-hydrogen bonds, van der Waals and pi-Alkyl, Alkyl interaction as depicted in **Figure 5.** The variation of interaction types between the potential inhibitors and the binding site residues was attributed to the different molecular features. Assessing the interaction profile of the reference (IMP-1088) compounds showed similar interaction types, as observed in **Figure 6**. The interactions observed herein include conventional and carbon-hydrogen bonds, van der Waals and pi-Alkyl, Alkyl interaction, pi-pi stacked, pi-pi T-shaped. Findings revealed similar interactions with binding site residue between the compounds and

the reference compound, suggesting CS1 and CS2 compounds may have the potential to elicit similar therapeutic effects against HsNMT1.

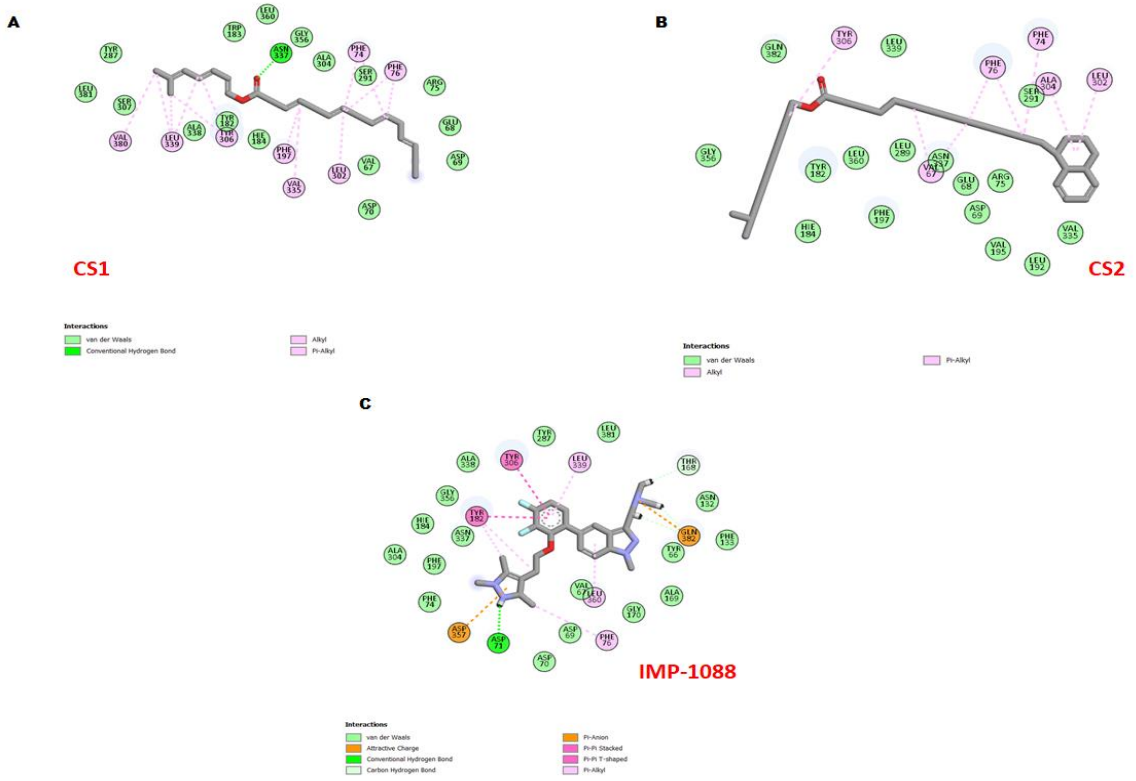

Figure 6: 2D molecular interactions of inhibitors A) CS1, B) CS2 and C) IMP-1088 within the binding site of the HsNMT1 showing similar interactions with the binding site residues suggesting the compounds have the potential to elicit similar therapeutic effects as reference IMP-1088.

The outcome of this investigation highlighted several possible biological activities; however, the selection of suitable biological activity was considered based on a higher Probable Activity (Pa) value over a probable inactivity value (Pi). Special attention was given to reported biological activity associated with the *SM* leaf extracts known to have antiviral activity. Thus the suitable biological activity predicted for the two isolated novel esters was antiviral activity, particularly towards rhinovirus. Amongst the selected targets, CS1 and CS2 showed a higher binding potential toward HsMNT1, an essential enzyme in treating the common cold. The MD simulation employed to test the effect of the compounds against HsNMT1 enzymes revealed that the compounds enacted good stability, flexibility, structural rigidity and reduced surface area exposed to solvents. These structural effects of the

compounds towards HsNMT1 were similar to the structural effects of the reference inhibitor, suggesting the potential inhibitory effects of the compounds toward HsNMT1.

In silico molecular recognition, protocols were employed to assess the pharmacological effects of the compounds CS1 and CS2 from the *SM* leaf. The predicted biological activity for the two isolated novel esters was anti-rhinovirus activity.

Molecular docking analysis indicated that CS1 and CS2 showed a higher binding potential toward HsMNT1. The MM/GBSA method revealed stronger binding free energy in CS1 and CS2 then the reference compound. Assessment of binding interactions also shows similarity in interactions CS1, CS2 and the reference IMP-1088 inhibitor, indicating the potential to elicit similar therapeutic effects against HsNMT.

CONCLUSION

The current study of the phytochemical analysis of DCM leaf extracts of SM led to the Identification of two esters that had previously not been reported in the plant. These compounds, 6-methylheptyl pentadecanoate and 6-methylheptyl-15-(1,2,3,4,4a,8a-hexahydronaphthalen-1-yl)pentadecanoate, possess anti-Rhino virus(HsNMT1) properties as indicated through an *in silico* molecular targeting prediction.

Further in vitro validation is required to optimize as a potential drug candidate.

Conflict of interest

The authors declare that they have no known competing financial interests or personal relationships that could have appeared to influence the work reported in this paper.

References

1. Sasidharan S, Chen Y, Saravanan D, Sundram K, Latha LY. Extraction, isolation and characterization of bioactive compounds from plants' extracts. African Journal of Traditional, Complementary and Alternative Medicines. 2011;8(1).
2. Anand U, Jacobo-Herrera N, Altemimi A, Lakhssassi N. A comprehensive review on medicinal plants as antimicrobial therapeutics: potential avenues of biocompatible drug discovery. Metabolites. 2019;9(11):258.
3. Mukherjee PK, Rai S, Kumar V, Mukherjee K, Hylands P, Hider R. Plants of Indian origin in drug discovery. Expert Opinion on Drug Discovery. 2007;2(5):633-57.
4. Balunas MJ, Kinghorn AD. Drug discovery from medicinal plants. Life sciences. 2005;78(5):431-41.
5. Mustafa G, Arif R, Atta A, Sharif S, Jamil A. Bioactive compounds from medicinal plants and their importance in drug discovery in Pakistan. 2017.
6. Osuntokun OT. Synergistic efficacy of Aframomum melegueta [Roscoe] K. Schum and Spondias mombin (Linn), A predictive treatment of SARS-CoV-2 (COVID-19) Infection. Journal of Bioscience & Biomedical Engineering (JB & Bio Engine. 2020;1(2):1-8.
7. Fred-Jaiyesimi A, Kio A, Richard W. α-Amylase inhibitory effect of 3β-olean-12-en-3-yl (9Z)-hexadec-9-enoate isolated from Spondias mombin leaf. Food Chemistry. 2009;116(1):285-8.
8. Corthout J, Pieters L, Claeys M, Berghe DV, Vlietinck A. Antiviral caffeoyl esters from Spondias mombin. Phytochemistry. 1992;31(6):1979-81.
9. Ojo OA, Afon AA, Ojo AB, Ajiboye BO, Oyinloye BE, Kappo AP. Inhibitory effects of solvent-partitioned fractions of two Nigerian herbs (Spondias mombin Linn. and Mangifera indica L.) on α-amylase and α-glucosidase. Antioxidants. 2018;7(6):73.
10. dos Santos Sampaio TI, de Melo NC, de Freitas Paiva BT, da Silva Aleluia GA, da Silva Neto FLP, da Silva HR, et al. Leaves of Spondias mombin L. a traditional anxiolytic and antidepressant: Pharmacological evaluation on zebrafish (Danio rerio). Journal of ethnopharmacology. 2018;224:563-78.
11. Cock IE, Van Vuuren SF. The traditional use of southern African medicinal plants in the treatment of viral respiratory diseases: A review of the ethnobotany and scientific evaluations. Journal of ethnopharmacology. 2020;262:113194.
12. Drysdale SB, Mejias A, Ramilo O. Rhinovirus–not just the common cold. Journal of Infection. 2017;74:S41-S6.
13. Revathi N, Dhanaraj T. Evaluation of bioactive phytochemicals in leaves extract of Dodonaea angustifolia using gas chromatography and mass spectroscopic technique. Journal of Pharmacognosy and Phytochemistry. 2019;8(3):4406-9.
14. Talukdar AD, Choudhury MD, Chakraborty M, Dutta B. Phytochemical screening and TLC profiling of plant extracts of Cyathea gigantea (Wall. Ex. Hook.) Haltt. and Cyathea brunoniana. Wall. ex. Hook (Cl. & Bak.). Assam University Journal of Science and Technology. 2010;5(1):70-4.
15. Uli H, Noor A, Mandey FW, Sapar A. Isolation, Identification and Bioactivity Test of Non Polar Compounds on N-hexane Extract of Haliclona (Reniera) Fascigera From Samalona Island-spermonde Archipelago. Marina Chimica Acta. 2016;17(2).
16. Varnek A, Tropsha A. Chemoinformatics approaches to virtual screening: Royal Society of Chemistry; 2008.
17. Lagunin A, Stepanchikova A, Filimonov D, Poroikov V. Internet server for on-line prediction of the biological activity spectrum for a substance. Bioinformatics. 2000;16(8):747-8.
18. Jairajpuri DS, Hussain A, Nasreen K, Mohammad T, Anjum F, Rehman MT, et al. Identification of natural compounds as potent inhibitors of SARS-CoV-2 main protease using combined docking and molecular dynamics simulations. Saudi Journal of Biological Sciences. 2021;28(4):2423-31.

19. Cheng Z, Wu T. TLC bioautography: high throughput technique for screening of bioactive natural products. Combinatorial chemistry & high throughput screening. 2013;16(7):531-49.
20. Djide MN. Sartini. Analisis Mikrobiologi Farmasi Makassar: Laboratorium Mikrobiologi Farmasi dan Bioteknologi Farmasi, Fakultas MIPA, Universitas Hasanudin. 2008.
21. Shaikh JR, Patil M. Qualitative tests for preliminary phytochemical screening: An overview. International Journal of Chemical Studies. 2020;8(2):603-8.
22. Pandith JI. Phytochemical screening of certain plant species of Agra city. Journal of drug delivery and therapeutics. 2012;2(4).
23. Hofmann MH, Gmachl M, Ramharter J, Savarese F, Gerlach D, Marszalek JR, et al. BI-3406, a Potent and Selective SOS1–KRAS Interaction Inhibitor, Is Effective in KRAS-Driven Cancers through Combined MEK InhibitionPan-KRAS SOS1 Protein–Protein Interaction Inhibitor BI-3406. Cancer discovery. 2021;11(1):142-57.
24. Berman HM, Westbrook J, Feng Z, Gilliland G, Bhat TN, Weissig H, et al. The protein data bank. Nucleic acids research. 2000;28(1):235-42.
25. Eric FP, Thomas DG, Conrad CH, Gregory SC, Daniel MG, Elaine CM, et al. UCSF Chimera? A visualization system for exploratory research and analysis. Journal of computational chemistry. 2004;25(13):1605-12.
26. Wiley J. Sons: Inc New York; NY; 2001.
27. Massova I, Kollman PA. Combined molecular mechanical and continuum solvent approach (MM-PBSA/GBSA) to predict ligand binding. Perspectives in drug discovery and design. 2000;18(1):113-35.
28. Genheden S, Kuhn O, Mikulskis P, Hoffmann D, Ryde U. The normal-mode entropy in the MM/GBSA method: effect of system truncation, buffer region, and dielectric constant. Journal of chemical information and modeling. 2012;52(8):2079-88.
29. Sitkoff D, Sharp KA, Honig B. Accurate calculation of hydration free energies using macroscopic solvent models. The Journal of Physical Chemistry. 1994;98(7):1978-88.
30. Ugadu AF, Ominyi M, Ogbanshi M, Eze U. Phytochemical analysis of Spondias mombin. international Journal of innovative Research and Development. 2014;3(9):101-7.
31. Sameh S, Al-Sayed E, Labib RM, Singab AN. Genus Spondias: A phytochemical and pharmacological review. Evidence-Based Complementary and Alternative Medicine. 2018;2018.
32. Quach HT, Steeper RL, Griffin GW. An improved method for the extraction and thin-layer chromatography of chlorophyll a and b from spinach. Journal of Chemical Education. 2004;81(3):385.
33. Sathya S. Separation of algal pigments by thin layer chromatography (TLC) and high performance liquid chromatography (HPLC). World Journal of Pharmaceutical Research. 2017;6:1275-84.
34. Sherma J, Fried B. Handbook of thin-layer chromatography: CRC press; 2003.
35. Hamberg M, Samuelsson B. Prostaglandin endoperoxides. Novel transformations of arachidonic acid in human platelets. Proceedings of the National Academy of Sciences. 1974;71(9):3400-4.
36. Wang Y, Han Y, Hu W, Fu D, Wang G. Analytical strategies for chemical characterization of bio-oil. Journal of separation science. 2020;43(1):360-71.
37. Baruah N, Dey SS, Nayak SK. Evaluation of dissolved gas analysis and long-term performance of non-edible natural ester. IEEE Transactions on Dielectrics and Electrical Insulation. 2020;27(5):1561-9.
38. Pratheeba T, Ragavendran C, Natarajan D. Larvicidal, pupicidal and adulticidal potential of Ocimum gratissimum plant leaf extracts against filariasis inducing vector. International journal of mosquito research. 2015;2(2):1-8.
39. Udo GJ, Etesin UM, Awaka-Ama JJ, Nyong AE, Uwanta EJ. GCMS and FTIR spectroscopy characterization of Luffa Cylindrica seed oil and biodiesel produced from the oil. Communication in Physical Sciences. 2010;5(1, 2, 3).

40. Socrates G. Infrared and Raman characteristic group frequencies: tables and charts: John Wiley & Sons; 2004.
41. Silverstein R. GC Bassler and TC Morrill, Sptrometric Identification of Organic Compounds. Wiley, NY; 1981.
42. Jain P, Soni A, Jain P, Bhawsar J. Phytochemical analysis of Mentha spicata plant extract using UV-VIS, FTIR and GC/MS technique. J Chem Pharm Res. 2016;8(2):1-6.
43. Karthikaiselvi R, Subhashini S. Study of adsorption properties and inhibition of mild steel corrosion in hydrochloric acid media by water soluble composite poly (vinyl alcohol-o-methoxy aniline). Journal of the Association of Arab Universities for Basic and Applied Sciences. 2014;16:74-82.
44. Pramila D, Xavier R, Marimuthu K, Kathiresan S, Khoo M, Senthilkumar M, et al. Phytochemical analysis and antimicrobial potential of methanolic leaf extract of peppermint (Mentha piperita: Lamiaceae). Journal of Medicinal Plants Research. 2012;6(2):331-5.
45. Rakhmatullin IZ, Efimov SV, Klochkov AV, Gnezdilov OI, Varfolomeev MA, Klochkov VV. NMR chemical shifts of carbon atoms and characteristic shift ranges in the oil sample. Petroleum Research. 2022;7(2):269-74.
46. Osuntokun OT, Idowu T, Gamberini MC. Bio-guided Isolation, Purification and Chemical Characterization of Epigallocatechin; Epicatechin, Stigmasterol, Phytosterol from of Ethyl Acetate Stem Bark Fraction of Spondias mombin (Linn.). 2018.
47. López-Camacho PY, Martínez-Espinosa JC, Basurto-Islas G, Torres-Zarraga A, Márquez-Villa JM, Macías-Alonso M, et al. Spondias mombin seed oil compounds identification by raman spectroscopy and NMR. Applied Sciences. 2021;11(6):2886.
48. Buckingham A. Chemical shifts in the nuclear magnetic resonance spectra of molecules containing polar groups. Canadian Journal of Chemistry. 1960;38(2):300-7.
49. Cao X, Lattao C, Pignatello JJ, Mao J, Schmidt-Rohr K. Sorption selectivity in natural organic matter probed with fully deuterium-exchanged and carbonyl-13C-labeled benzophenone and 1H–13C NMR spectroscopy. Environmental science & technology. 2014;48(15):8645-52.
50. Wu Q, Yu S, Hao N, Wells Jr T, Meng X, Li M, et al. Characterization of products from hydrothermal carbonization of pine. Bioresource technology. 2017;244:78-83.
51. Neiens SD, Geißlitz SM, Steinhaus M. Aroma-active compounds in Spondias mombin L. fruit pulp. European Food Research and Technology. 2017;243(6):1073-81.
52. Zheng C, Zhu M, Zhang D. Characterisation of asphaltenes extracted from an Indonesian oil sand using NMR, DEPT and MALDI-TOF. Energy Procedia. 2015;75:847-52.
53. David AA, Oladele AA, Philip AO, Zabdiel AA, Olufunso AB, Tolulope OO, et al. Tropical Journal of Natural Product Research. 2022.
54. Elufioye TO, Obuotor EM, Agbedahunsi JM, Adesanya SA. Anticholinesterase constituents from the leaves of Spondias mombin L.(Anacardiaceae). Biologics: targets & therapy. 2017;11:107.
55. Echeme JO, Ahuchogu AA, Uchegbu RI. Spondias mombin linn. American Journal of Chemistry and Applications. 2014;1(3):28-31.
56. Huynh T, Smith JC, Sanson A. Protein unfolding transitions in an intrinsically unstable annexin domain: Molecular dynamics simulation and comparison with nuclear magnetic resonance data. Biophysical journal. 2002;83(2):681-98.
57. Osuntokun O, Ige O, Idowu T, Gamberini M. Bio-activity and Spectral Analysis of Gas Chromatography/Mass Spectroscopy (GCMS) Profile of Crude Spomdias mombin Extracts. SciFed Journal of Analytical Biochemistry. 2018;1(2):1-12.
58. Fred-Jaiyesimi AA, Wilkins RM, Abo KA. Glucose lowering activities of mombintane I and mombintane II isolated from the leaves of Spondias mombin L. International Journal of Biological and Chemical Sciences. 2017;11(3):1315-9.
59. Kufareva I, Abagyan R. Methods of protein structure comparison. Homology modeling: Springer; 2011. p. 231-57.

60. MIu L, Bogatyreva N, Galzitskaia O. Radius of gyration is indicator of compactness of protein structure. Molekuliarnaia biologiia. 2008;42(4):701-6.
61. Durham E, Dorr B, Woetzel N, Staritzbichler R, Meiler J. Solvent accessible surface area approximations for rapid and accurate protein structure prediction. Journal of molecular modeling. 2009;15(9):1093-108.
62. Tiwari A, Mukherjee B, Dixit M. MicroRNA key to angiogenesis regulation: miRNA biology and therapy. Current cancer drug targets. 2018;18(3):266-77.
63. Xue J, Huang X, Zhu Y. Using molecular dynamics simulations to evaluate active designs of cephradine hydrolase by molecular mechanics/Poisson–Boltzmann surface area and molecular mechanics/generalized Born surface area methods. RSC advances. 2019;9(24):13868-77.
64. Salifu EY, Issahaku AR, Agoni C, Ibrahim MA, Manimbulu N, Soliman ME. Prioritizing the Catalytic Gatekeepers through Pan-Inhibitory Mechanism of Entrectinib against ALK, ROS1 and TRKA Tyrosine Kinases. Cell Biochemistry and Biophysics. 2022;80(1):11-21.
65. Salifu EY, Agoni C, Soliman ME. Highlighting the mechanistic role of Olutasidenib (FT-2102) in the selective inhibition of mutated isocitrate dehydrogenase 1 (mIDH1) in cancer therapy. Informatics in Medicine Unlocked. 2022;28:100829.
66. Genheden S, Ryde U. The MM/PBSA and MM/GBSA methods to estimate ligand-binding affinities. Expert opinion on drug discovery. 2015;10(5):449-61.
67. Durrant JD, McCammon JA. Molecular dynamics simulations and drug discovery. BMC biology. 2011;9(1):1-9.

Supplementary materials

Structures and anti-Rhino virus properties of 6-methylheptyl pentadecanoate and 6-methylheptyl 15-(1,2,3,4,4a,8a-hexahydronaphthalen-1-yl)pentadecanoate against HsNMT1 protein target, from Leaf Extract of *Spondias mombin Linn*

Supplementary Table TS1: FTIR Analysis of compounds CS1 and CS2

Absorption Wavelength (cm^{-1})	Literature Wavelength (cm^{-1})	Intensity	Functional Group	Compound Type
725.0	715-725	m-w	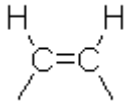	Alkanes and Alkyls
1220.0	1160-1210	s-vs	C-O	Aliphatic esters O=C-O-C With two bands,1 stronger than the other
1465.0	1450-1470	s	C-H (bending)	Alkyls
1748.0	1750-1735	vs	C=O	Carbonyl (ester C=O Stretch) Membrane lipid, fatty acid
2927.0	2850-3000	s	C-H stretch	Alkyls

Intensity key: vw = very weak, w = weak, m = medium, s = strong, vs = very strong

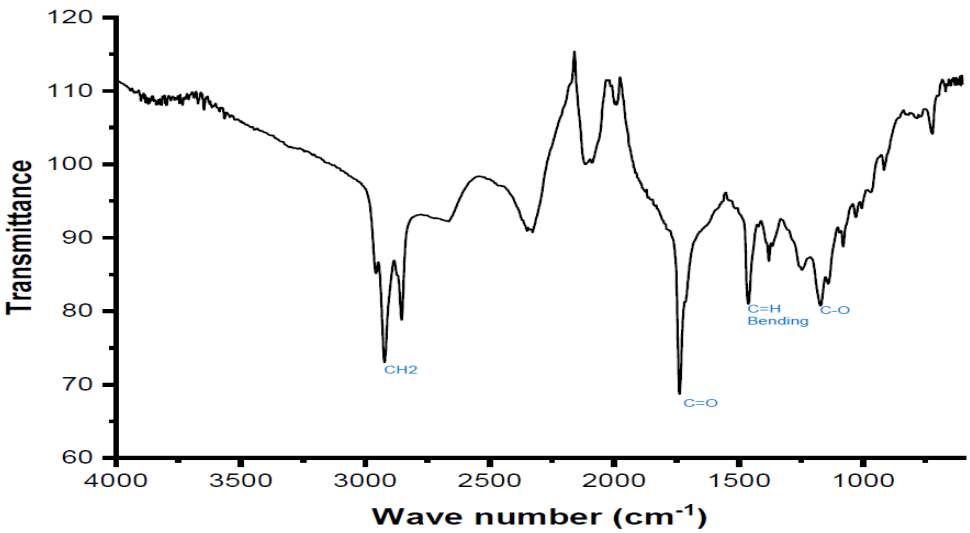

Figure S1: FTIR chromatogram of CS1

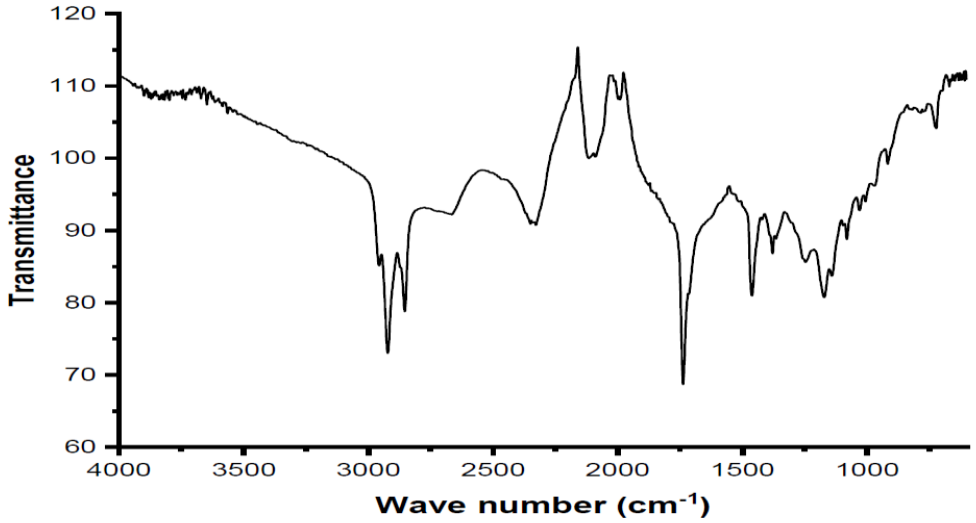

Figure S2: FTIR chromatogram of CS2

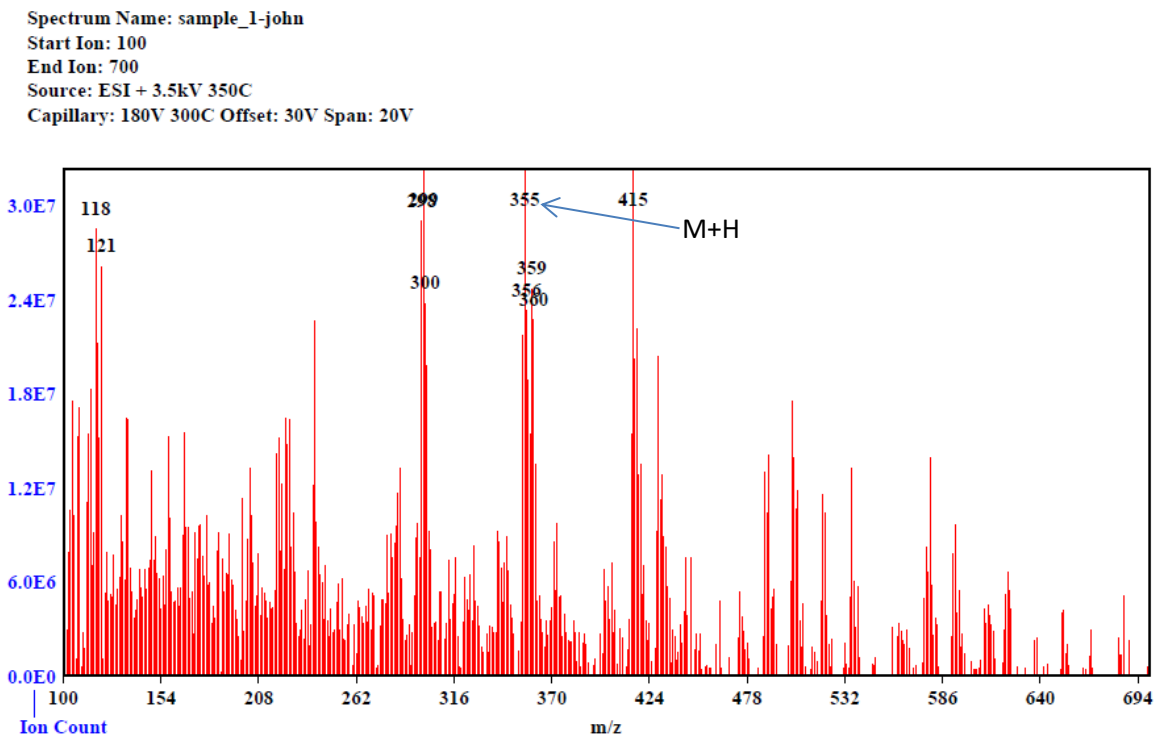

Figure S3: Mass spectrum of CS1

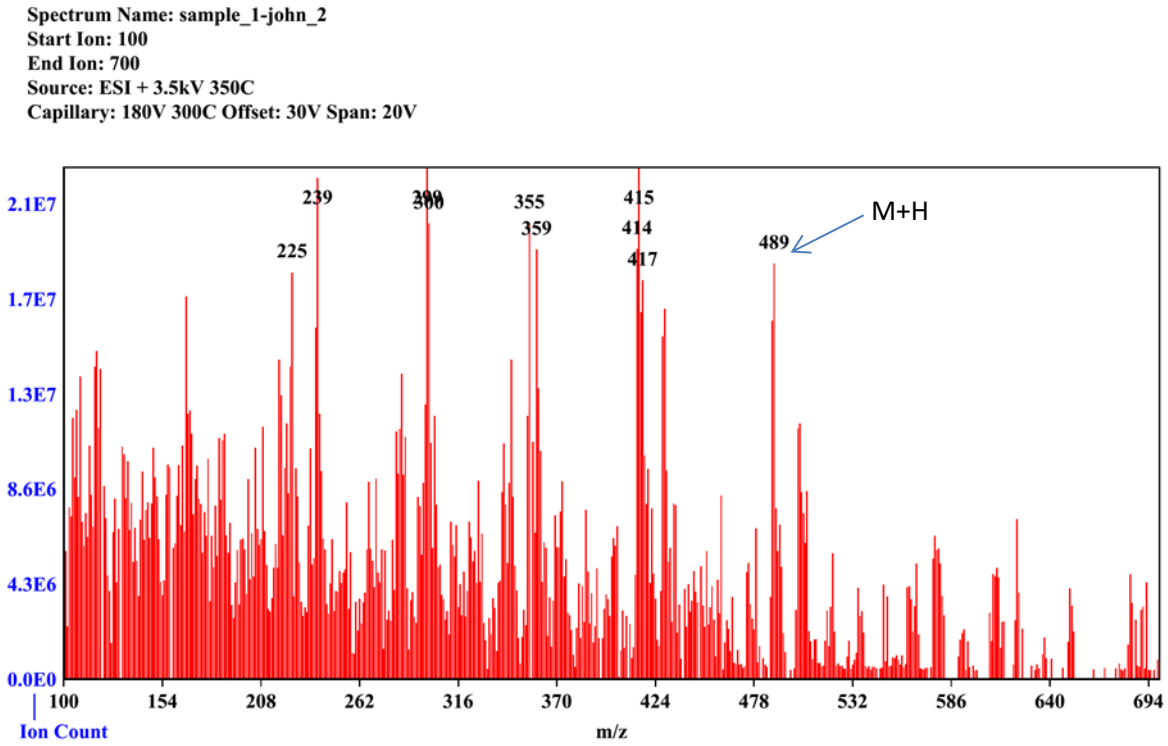

Figure S4: Mass spectrum of CS2

Supplementary Table 2- TS2: Proton 1H NMR Analysis of compound CS1

Carbon No.	δ^1**H** (ppm)	δ^1**H** C (ppm) literature	**Functional Group**	**Compound Type**
1	1.30	0.8-1.6	CH_2-CH_2-	Aliphatic alkane
2	1.70		CH_2-CH_2-	Aliphatic alkane
3	1.50	0.8-1.6	CH_3-CH_2-	Aliphatic alkane
4	0.90	0.8-1.6	CH_2-CH_2-	Aliphatic alkane
8	3.90	3.5-4.8	-OCH_2	Alkyl of ester
10	2.30	2.0-3.0	O=C-CH_2	Proton/Alkyl adjacent to carbonyl

Supplementary Table 3- TS3: Carbon 13 NMR Analysis of compound CS1

Carbon No.	δ13C (ppm)	δ13C (ppm) literature	**Functional Group**	**Compound Type**
1	10.97	10-40	CH_3	Aliphatic hydrocarbon
2	14.03-14.11	10-40	CH_2	Aliphatic hydrocarbon
3	22-25	10-40	CH_3	Aliphatic hydrocarbon
4	30	10-40	CH_2	Aliphatic hydrocarbon
5	32	10-40	CH_2	Aliphatic hydrocarbon
6	35	10-40	CH_2	Aliphatic hydrocarbon
7	36	10-40	CH_2	Aliphatic hydrocarbon
8	40	37.0–60.0	CH_2	Methine (CH) group in alkyl fragments; CH and CH_2 alkyl groups of naphthenic fragments, adjacent to CH group
9	68	62-69	CH_2O	Glyceryl ester
10	79	-	C-C=O	Carbon next to the carbonyl of ester
11	173.57	180–163	C=O	Ester, carboxylic acid

Supplementary Table 4- TS4 Proton (^{1}H) NMR Analysis of compound CS2

Carbon No.	δ^1**H** (ppm)	δ^1**H** C (ppm)literature	**Functional Group**	**Compound Type**
1	1.21	0.8-1.6	$-CH_3$	Aliphatic alkane
2	4.20	3.5-4.8	$-OCH_2$	Alkyl of ester
3	-	-	C=O	C=O of ester (no proton)
4	2.88	2.0-3.0	CH	Proton next to C=O
5	7.66	-	=CH	Cyclic alkene
6	7.29	4.0-7.3	HC=CH	alkene
7	6.64	4.0-7.3	HC=CH	alkene
8	5.80	-	=C-CH	Proton next to alkene
9	2.68	2.0-3.0	-CH	Proton next to C=O/alkene
10	1.25	0.8-1.6	$-CH_2$	Aliphatic alkane
11	1.25	0.8-1.6	$-CH_2$	Aliphatic alkane
12	1.25	0.8-1.6	$-CH_2-CH_2$	Aliphatic alkane
13	1.26	0.8-1.6	$-CH_2-CH_2$	Aliphatic alkane
14	1.26	0.8-1.6	$-CH_2-CH_2$	Aliphatic alkane
15	1.25	0.8-1.6	$-CH_2-CH_2$	Aliphatic alkane
16	1.25	0.8-1.6	$-CH_2-CH_2$	Aliphatic alkane
17	1.19	0.8-1.6	$-CH_2-CH$	Aliphatic alkane
18	1.50	1.2-1.7	$CH_2-CH-CH_2$	Cyclic alkane
19	1.63,1.38	1.2-1.7	$CH-CH_2-CH_2$	Cyclic alkane
20	1.63,1.38	1.2-1.7	CH_2-CH_2-CH	Cyclic alkane
21	1.24	1.2-1.7	$CH-CH_2$	Cyclic alkane
22	1.45,1.20	1.2-1.7	$CH-CH_2-CH$	Cyclic alkane
23	1.54	1.2-1.7	$CH_2-CH-CH_3$	Cyclic alkane
24	0.86	-	$-CH-CH_3$	Alkyl attached to a non- aromatic cyclic ring
25	1.63,1.38	1.2-1.7	$CH_2-CH-CH_2$	Cyclic alkane
26	1.63,1.38	1.2-1.7	$CH-CH_2-CH_2$	Cyclic alkane
27	1.24	1.2-1.7	$CH-CH_2$	Cyclic alkane
28	1.45,1.20	1.2-1.7	$CH-CH_2-$ CH	Cyclic alkane

Supplementary Table 5- TS5: Carbon 13 NMR Analysis of compound CS2

Carbon No.	δ13C (ppm)	δ13C (ppm) literature	**Functional Group**	**Compound Type**
1	10.98	10-40	$-CH_3$	Aliphatic hydrocarbon
2	14.04	10-40	-CH-	Aliphatic hydrocarbon
3	14.11	10-40	$-CH_3$	Aliphatic hydrocarbon
4	22.69	10-40	$-CH_2$	Aliphatic hydrocarbon
5	22.96	10-40	$-CH_2$	Aliphatic hydrocarbon
6	23.79	10-40	$-CH_2$	Aliphatic hydrocarbon
7	24.48	10-40	$-CH_2$	Aliphatic hydrocarbon
8	66.81	62-69	$-OCH_2-$	Ester
9	173.57	180–163	-OCO-	Ester
10			$-CH_3COO-$	CH_3 attached to the carbon of ester
11	28.92	10-40	CH_2	Aliphatic hydrocarbon
12	29.36	10-40	CH_2	Aliphatic hydrocarbon
13	29.66	10-40	CH_2	Aliphatic hydrocarbon
14	29.70	10-40	CH_2	Aliphatic hydrocarbon
15	30.41	10-40	CH_2	Aliphatic hydrocarbon
16	31.93	10-40	CH_2	Aliphatic hydrocarbon
17	34.00	10-40	CH_2	Aliphatic hydrocarbon
18	38.74	10-40	CH_2	Aliphatic hydrocarbon
19		10-40	CH_2	Aliphatic hydrocarbon
20		10-40	CH_2	Aliphatic hydrocarbon
21		10-40	CH_2	Aliphatic hydrocarbon
22		10-40	CH_2	Aliphatic hydrocarbon
23		10-40	$-CH_2$	Aliphatic hydrocarbon
24		10-40	-CH-	Cyclic alkane
25		10-40	$-CH_2$	Cyclic alkane
26		10-40	$-CH_2$	Cyclic alkane
27		10-40	$-CH_2$	Cyclic alkane
28		20-50	-CH-	Cyclic alkane
29		20-50	-CH-	Cyclic alkane
30	114.03	80-150	=CH	Cyclic alkene
31	127.58	80-150	=CH	Cyclic alkene
32	127.58	80-150	=CH	Cyclic alkene
33	127.58	80-150	=CH	Cyclic alkene

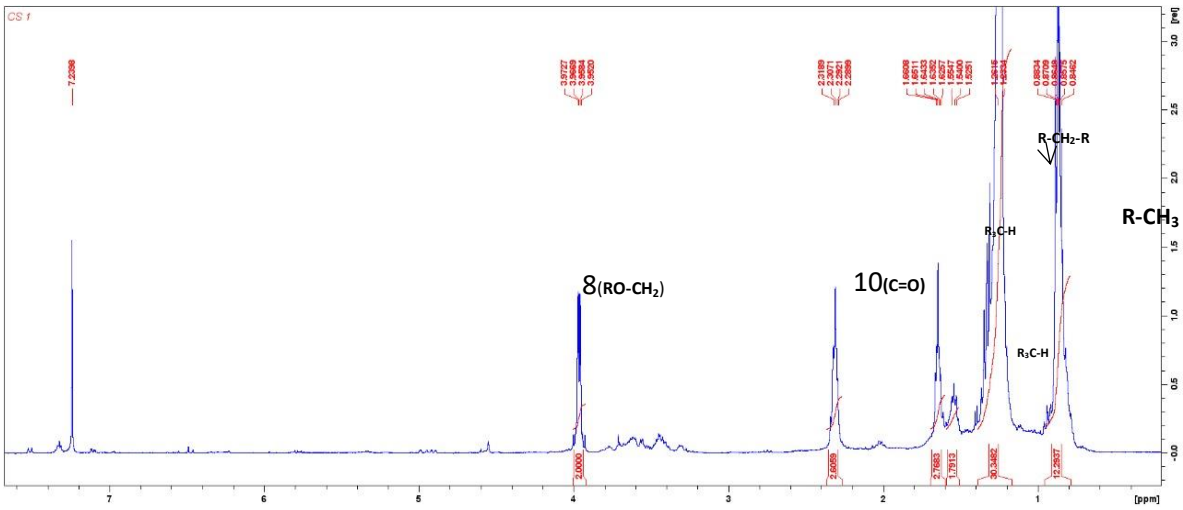

Figure S5: Proton (^{1}H) NMR Spectrum of compound CS1

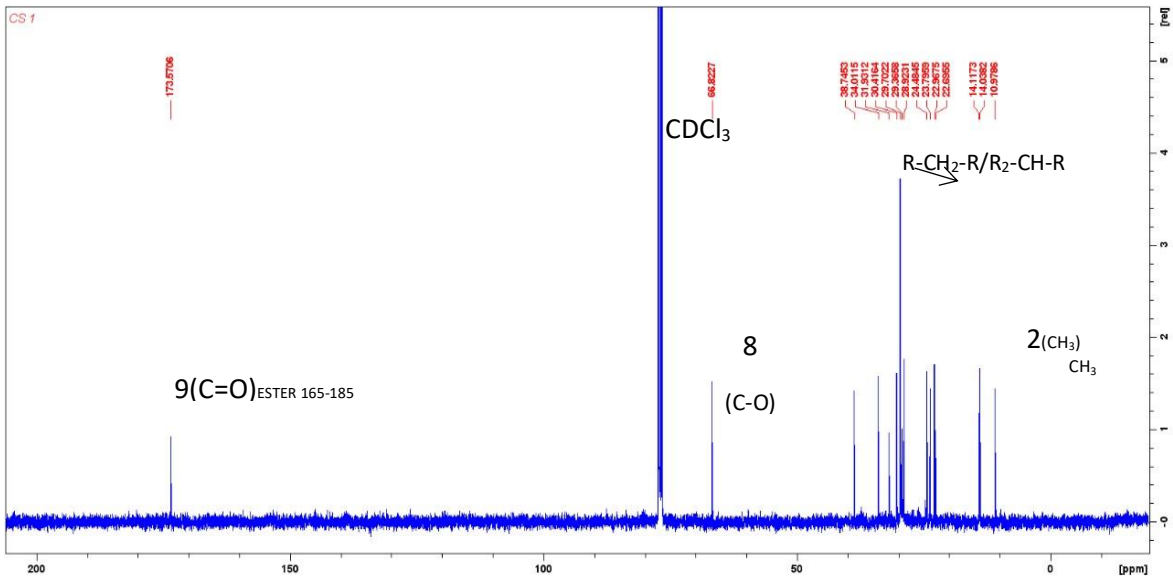

Figure S6: Carbon 13 NMR Analysis of compound CS1

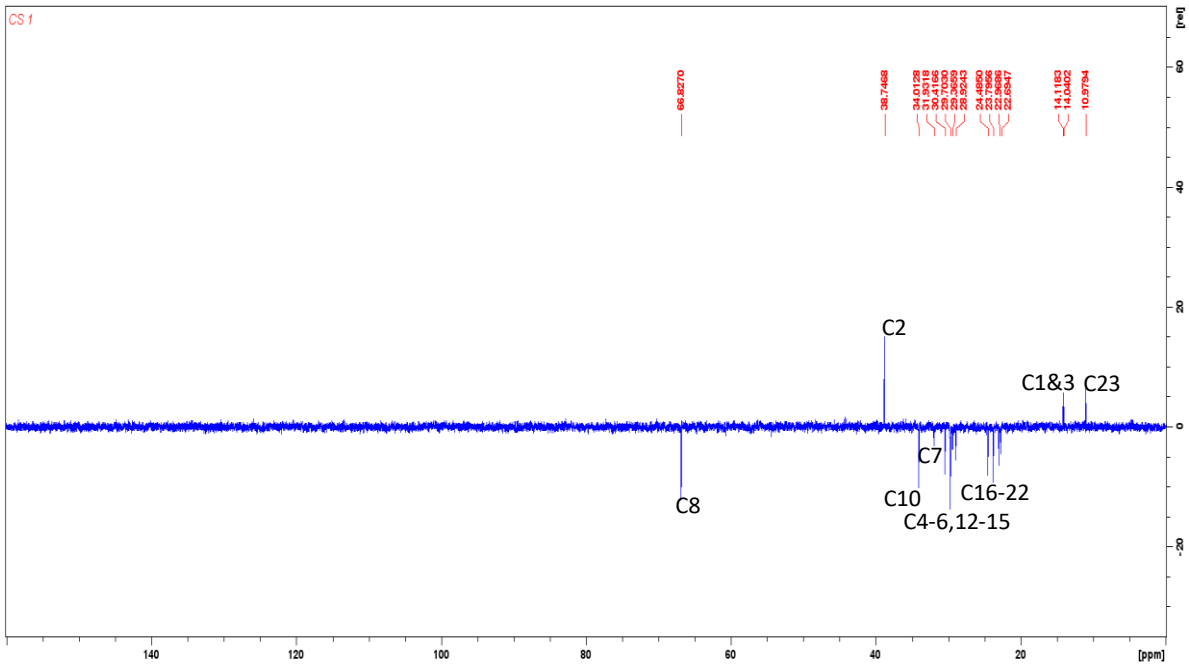

Figure S7: DEPT-135 spectrum of CS1

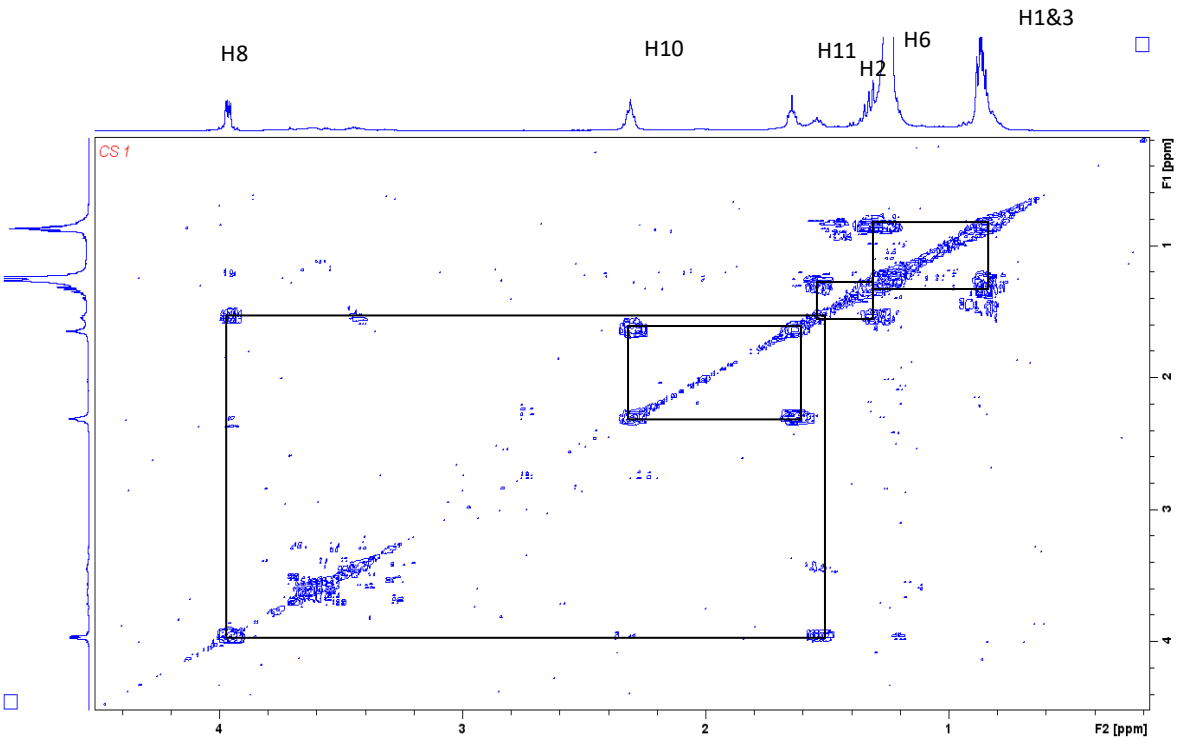

Figure S8: COSY Spectrum of CS1

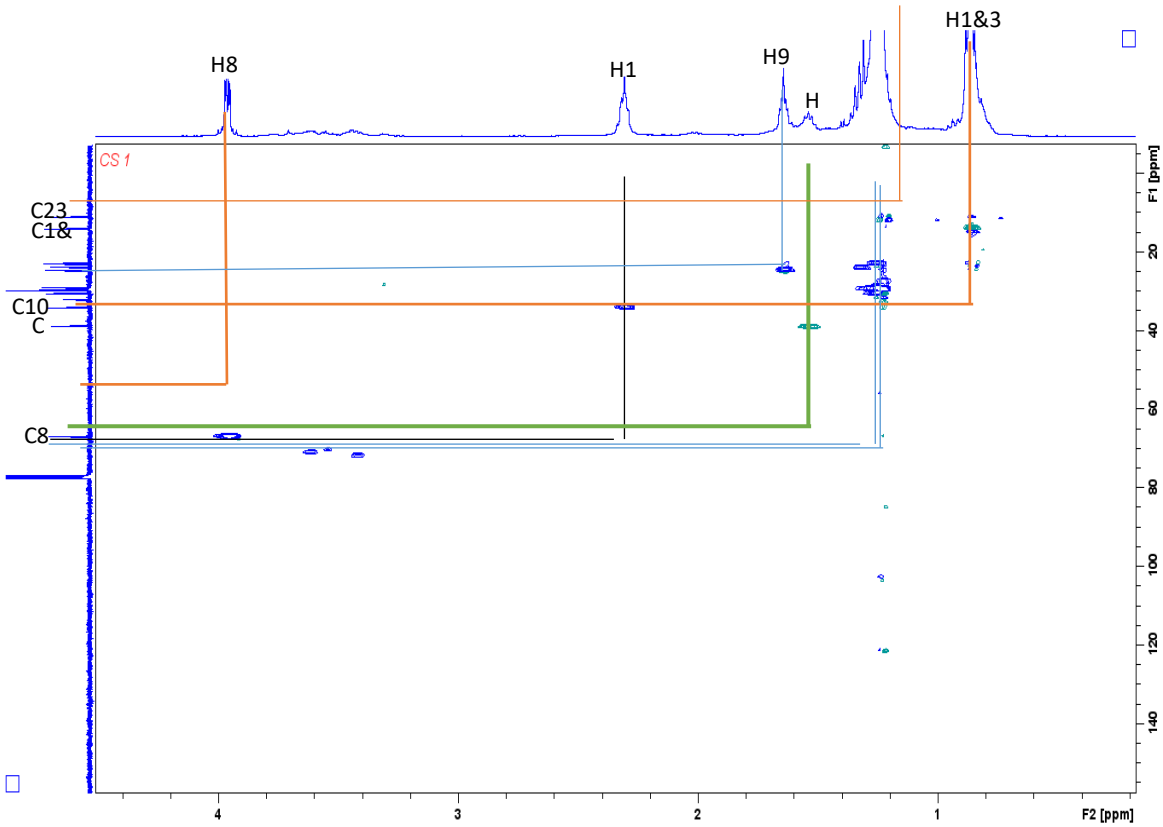

Figure S9: HSQC spectrum of CS1

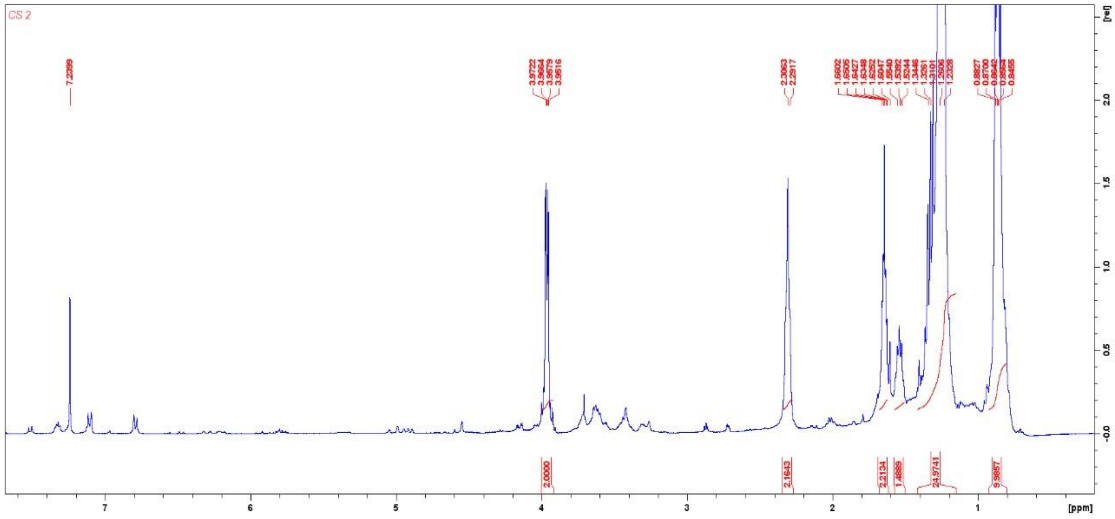

Figure S10: Proton (^{1}H) NMR Spectrum of compound CS2

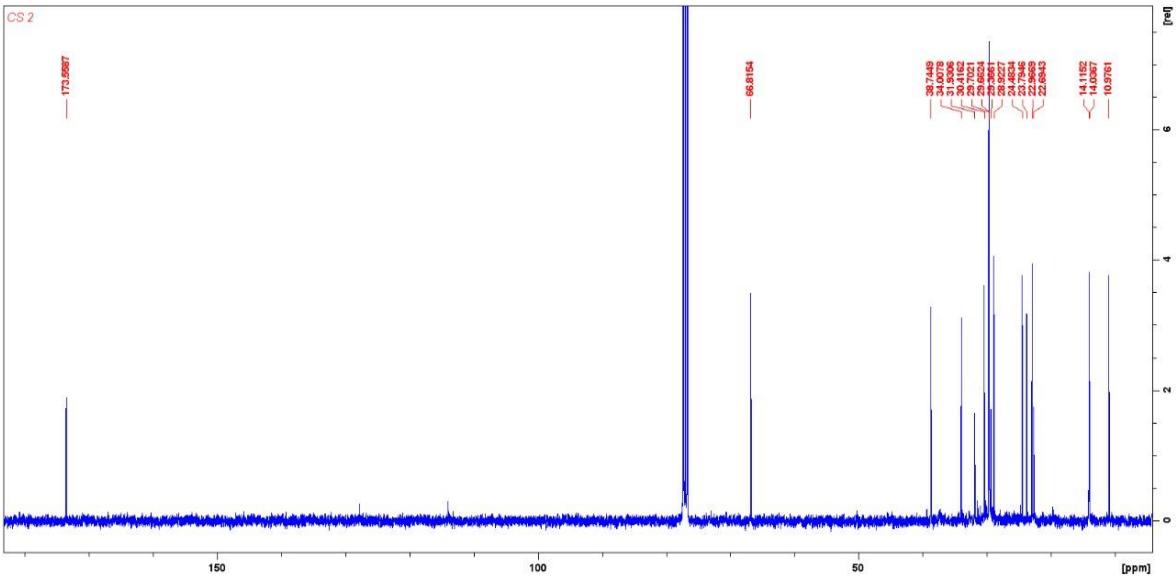

FIGURE S11: carbon 13 NMR Spectrum of compound CS2

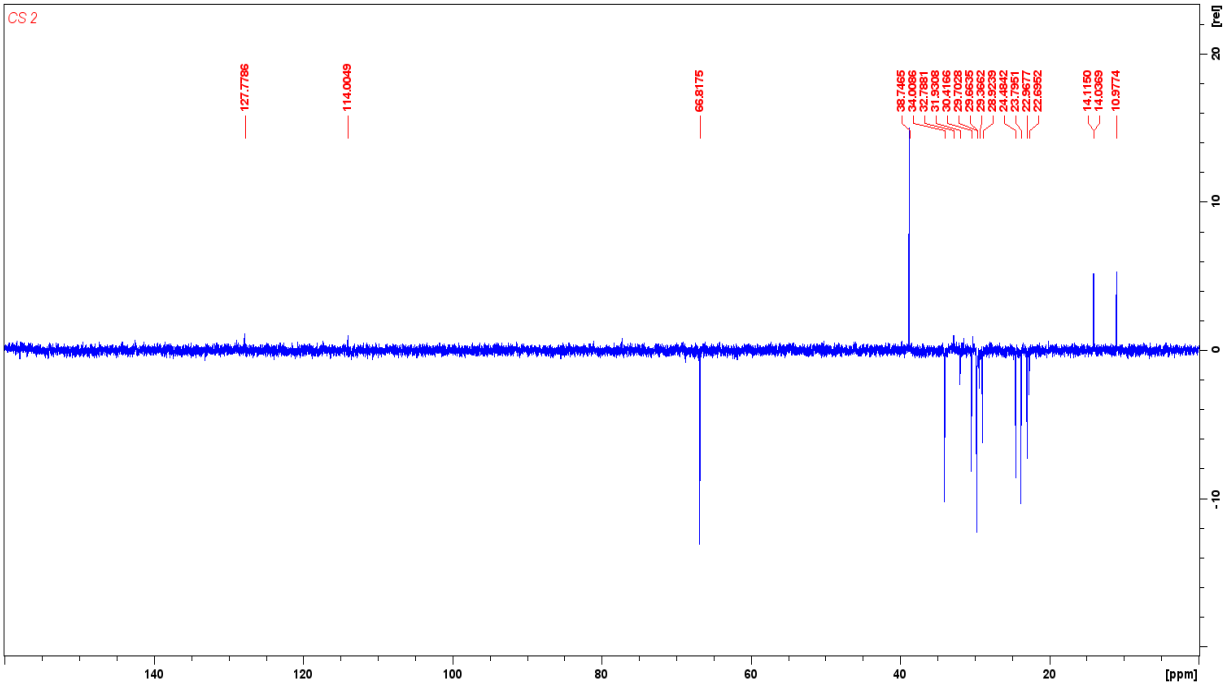

Figure S12: DEPT-135 spectrum of CS2

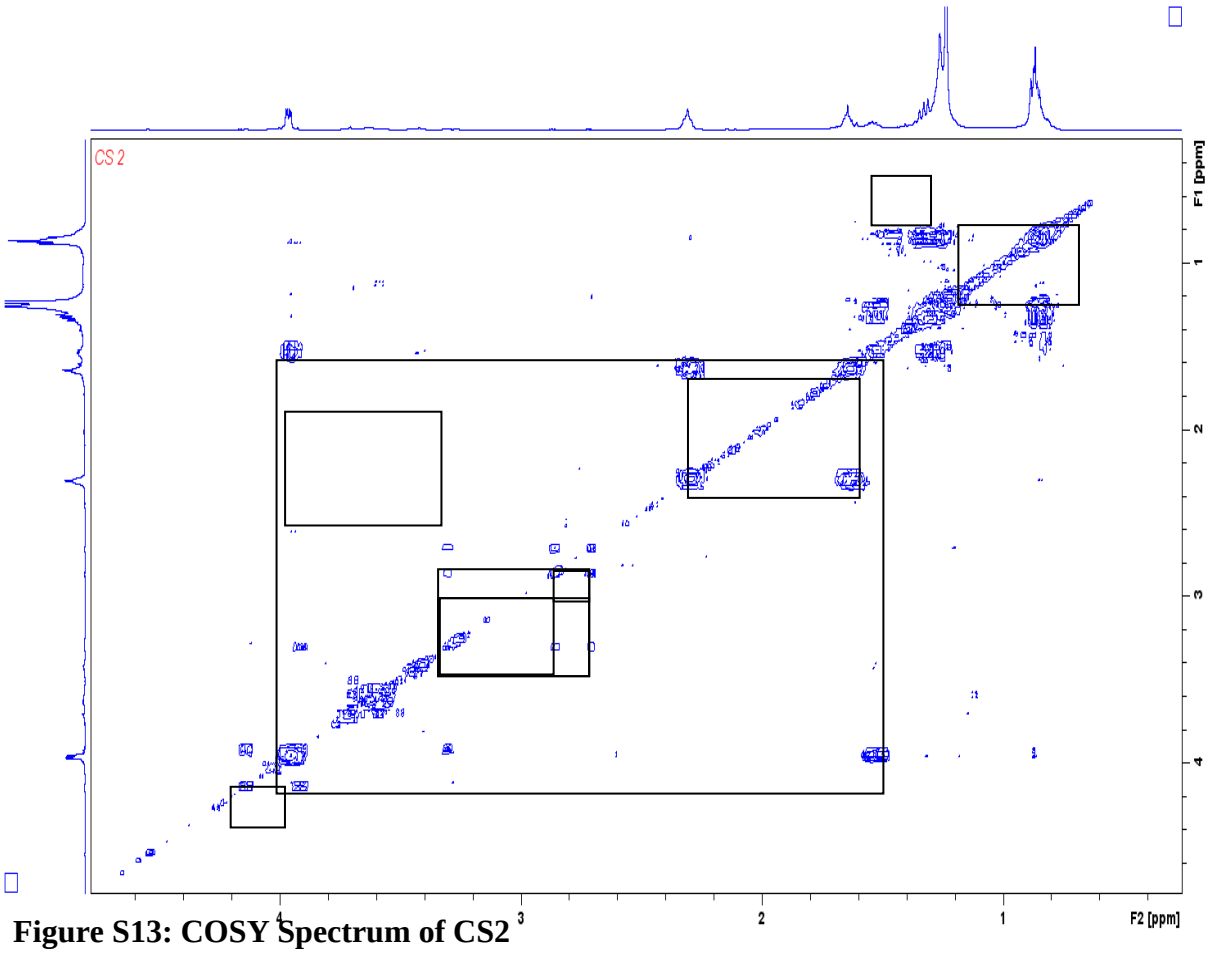

Figure S13: COSY Spectrum of CS2

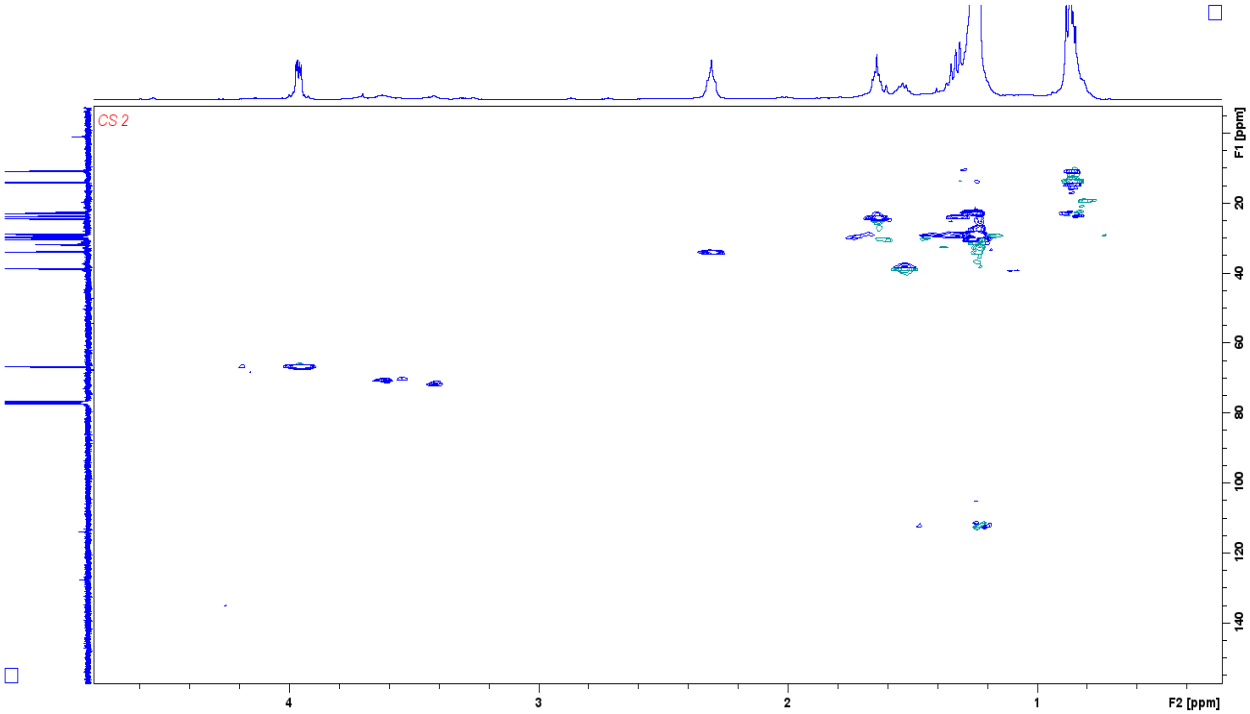

Figure S14: HSQC Spectrum of CS2